

NACA RM No. L8B02



JUN 1948

NACA

RESEARCH MEMORANDUM

AERODYNAMIC CHARACTERISTICS OF SEVERAL
NACA AIRFOIL SECTIONS AT SEVEN REYNOLDS
NUMBERS FROM 0.7×10^6 TO 9.0×10^6

By

Laurence K. Loftin, Jr., and M. Irene Poteat

Langley Memorial Aeronautical Laboratory
Langley Field, Va.

**NATIONAL ADVISORY COMMITTEE
FOR AERONAUTICS**

WASHINGTON

May 27, 1948

NACA LIBRARY
LANGLEY MEMORIAL AERONAUTICAL
LABORATORY
LANGLEY FIELD, VA.

NATIONAL ADVISORY COMMITTEE FOR AERONAUTICS

RESEARCH MEMORANDUM

AERODYNAMIC CHARACTERISTICS OF SEVERAL
NACA AIRFOIL SECTIONS AT SEVEN REYNOLDS
NUMBERS FROM 0.7×10^6 TO 9.0×10^6

By Laurence K. Loftin, Jr., and M. Irene Poteat

SUMMARY

An investigation has been made of the two-dimensional aerodynamic characteristics of several NACA airfoil sections at four Reynolds numbers from 2.0×10^6 to 0.7×10^6 . The group of airfoils tested consisted of four NACA 64-series sections varying in thickness from 9 percent to 18 percent and having design lift coefficients of 0.4, and two NACA 230-series sections of 12-percent and 15-percent thickness. Aerodynamic data for the range of Reynolds numbers from 2.0×10^6 to 0.7×10^6 were obtained for each of these airfoils, both with and without split flaps, in the smooth condition and with roughened leading edges. The results of this investigation, together with previously published data for the same airfoils at Reynolds numbers of 9.0, 6.0, and 3.0×10^6 , are included in the present paper.

The minimum drag of each of the smooth airfoils increased progressively as the Reynolds number was lowered from 9.0×10^6 to 0.7×10^6 . The magnitude of this increase appeared to become larger as the thickness ratio of the NACA 64-series airfoils was increased. Decreasing the Reynolds number from 9.0×10^6 to 0.7×10^6 caused a reduction in the maximum lift of all the airfoils both in the smooth condition and with rough leading edges. The magnitude and character of this reduction, however, varied with airfoil design and surface condition so that the comparative merits of the various airfoils changed markedly with Reynolds number and surface condition. Although the results are not entirely consistent, some decreases in the lift-curve slope of both the smooth and rough airfoils usually accompanied a reduction in Reynolds number. Both the angle of zero lift and the pitching moment appeared to be nearly independent of the Reynolds number.

INTRODUCTION

Two-dimensional aerodynamic data corresponding to Reynolds numbers of 3.0, 6.0, and 9.0×10^6 are now generally available (reference 1) for a rather large number of systematically derived NACA 6-series and 4- and 5-digit-series airfoil sections. Although the range of Reynolds number covered by the investigation reported in reference 1 is reasonably wide, engineering problems such as may be encountered in the design of personal-type aircraft and helicopter blades may require data for a range of Reynolds numbers extending below 3.0×10^6 .

With a view toward providing a basis upon which to choose airfoils for such applications, an experimental investigation has been made of the aerodynamic characteristics of a number of NACA airfoils at Reynolds numbers varying from 2.0×10^6 to 0.7×10^6 . The results of this investigation are presented in the present paper, together with the higher Reynolds number data of reference 1 for the same airfoils.

The airfoils for which data are presented include four NACA 64-series sections, cambered for design lift coefficients of 0.4, and two NACA 5-digit-series sections, the NACA 23012 and NACA 23015. The lift, drag, and pitching-moment characteristics are presented for each of the smooth, plain airfoils at seven Reynolds numbers from 0.7×10^6 to 9.0×10^6 . A sufficient amount of data is also presented to show the scale effect upon the characteristics of the airfoils with roughened leading edges and simulated split flaps.

SYMBOLS

c_d	section drag coefficient
c_l	section lift coefficient
c_{l_i}	section design lift coefficient
$c_{l_{max}}$	maximum section lift coefficient
$c_{m_c/4}$	section pitching-moment coefficient about quarter-chord point
c_{mac}	section pitching-moment coefficient about aerodynamic center
α_0	section angle of attack

$dc_l/d\alpha_0$ section lift-curve slope

R Reynolds number, based on airfoil chord and free-stream velocity

AIRFOILS

The airfoil sections for which experimental results were obtained are:

NACA 64-409

NACA 64₁-412

NACA 64₂-415

NACA 64₃-418

NACA 23012

NACA 23015

These airfoils were chosen for investigation because, on the basis of the data of reference 1, they appeared to offer the best possibilities for applications where the requirements call for low drag, high lift, and moderate pitching moments, and where compressibility effects are negligible. Complete descriptions of these airfoil sections, including the methods of derivation and theoretical pressure-distribution data, are available in reference 1. The ordinates of the six airfoils tested are presented in table I.

APPARATUS AND TESTS

Models.- The 24-inch chord models of the six airfoil sections tested were constructed of laminated mahogany. The surfaces of the models were painted with lacquer and then sanded with number 400 carborundum paper until aerodynamically smooth.

Wind tunnel and test methods.- The experimental investigation was made in the Langley two-dimensional low-turbulence tunnel (LTT). The test section of this tunnel measures 3 feet by 7.5 feet with the models, when mounted, completely spanning the 3-foot dimension. The Reynolds number is varied by means of the tunnel airspeed since this tunnel operates at atmospheric pressure only. Lift measurements are usually made in this tunnel by taking the difference of the integrated pressure reaction upon the floor and ceiling of the tunnel (reference 2). Because of the small dynamic pressures employed in the present

investigation, however, more accurate measurements of the lift were obtainable with the three-component balance which is part of the equipment of the low-turbulence tunnel. The balance was therefore used for the lift and pitching-moment tests in the present investigation.

For tests using the balance, the models were supported in the tunnel on trunnions extending through the tunnel walls from the balance frame. A small gap was allowed between the ends of the model and the tunnel walls to insure freedom of movement of the balance. Since air leakage through these gaps was considered as a possible source of error, lift tests were made at Reynolds numbers of 2.0×10^6 and 1.5×10^6 with the gaps first open and then sealed. The measurements for the gaps-sealed condition were made with the tunnel floor and ceiling pressure orifices, and for the gaps-open tests, the balance was used. Results obtained by the two methods agreed to within the experimental error for these Reynolds numbers and would be expected to agree equally well at the lower Reynolds numbers.

Comparative tests showed that more accurate measurements of the drag were possible with the wake-survey apparatus than with the balance. Hence, all drag measurements were made by the wake-survey method (reference 2) with the gaps between the model and tunnel walls sealed.

Tests.- The tests of each smooth airfoil consisted of measurements of the lift, drag, and quarter-chord pitching moment at Reynolds numbers of 2.0×10^6 , 1.5×10^6 , 1.0×10^6 , and 0.7×10^6 . In none of the tests did the Mach number exceed 0.15. Lift and moment measurements at each of the four Reynolds numbers were also made of the airfoils equipped with 0.20c simulated split flaps (reference 1) deflected 60° . In addition, all of the measurements except those of the pitching moment were repeated with standard roughness applied to the leading edges of the airfoils. The standard roughness employed was the same as that used in previous investigations (reference 1) and consisted of 0.011-inch-diameter carborundum grains spread over a surface length of 8 percent of the chord back from the leading edge on the upper and lower surfaces of the airfoil. The grains were thinly spread to cover from 5 to 10 percent of this area.

Supplementary tests were made in the Langley two-dimensional low-turbulence pressure tunnel (TDT) at a Reynolds number of 6.0×10^6 of the NACA 23012 and NACA 23015 equipped with split flaps. Such data are available in reference 1 for the other airfoils tested in the present investigation, and were considered necessary for the NACA 23012 and NACA 23015 in order to compare adequately the type of scale effect shown by these airfoils with that of the other four.

RESULTS

The results are presented (figs. 1 to 6) in the form of standard aerodynamic coefficients representing the lift, drag, and quarter-chord pitching moment. The Reynolds number range for which the plain airfoil data are presented extends from 9.0×10^6 to 0.7×10^6 and includes the data obtained in the present investigation for four Reynolds numbers from 2.0×10^6 to 0.7×10^6 , and those from reference 1 for three Reynolds numbers from 9.0×10^6 to 3.0×10^6 . Data are presented for the airfoils with split flaps and with roughened leading edges at five Reynolds numbers from 6.0×10^6 to 0.7×10^6 . From the quarter-chord pitching-moment data, the position of the aerodynamic center and the variation of the moment about this point were calculated and are presented.

The influence of the tunnel boundaries has been removed from all the aerodynamic data by means of the following equations (developed in reference 2):

$$c_d = 0.990c_d'$$

$$c_l = 0.973c_l'$$

$$c_{m_c}/4 = 0.951c_{m_c}/4'$$

$$\alpha_o = 1.015\alpha_o'$$

where the primed quantities represent the coefficients measured in the tunnel.

DISCUSSION

Insofar as the scope of the experimental data permits, an analysis has been made of the effect of several airfoil parameters upon the way in which the important aerodynamic characteristics of the airfoils vary with Reynolds number. As an aid to this analysis, cross plots are used showing some of the aerodynamic characteristics of the airfoils as a function of Reynolds number.

Drag.- The general form of the drag polars corresponding to the various Reynolds numbers may be seen in figures 1 to 6. The principal effects on the drag of decreasing the Reynolds number from 9.0×10^6

to 0.7×10^6 appear to be a variation in width of the flat portion of the drag polars, an increase in value of the minimum drag coefficient, and a steepening of the drag curves beyond the flat portion of the polars.

The extent of the lift-coefficient range over which the NACA 64-series sections have low drag, corresponding to extensive laminar flow on the airfoil surfaces, generally increases as the Reynolds number is lowered. The greatest increase is evident in the results for the 18-percent-thick section, but the amount of data available is not sufficient to show whether or not the amount of increase varies in a consistent manner with airfoil-thickness ratio. Following reductions in the Reynolds number below 2.0×10^6 , some increase of drag with lift coefficient within the low-drag range is shown by the results for all the airfoils and is particularly pronounced in the drag polars for the NACA 64₂-415 section (fig. 3). Unpublished data obtained at the Langley Laboratory have shown this behavior to be related to the formation at the lower Reynolds numbers of a laminar separation bubble behind the position of minimum pressure on the upper surface of the airfoil. The increase of drag with lift in the low-drag range is explained by an increase in size of the bubble which is caused by the progressively more unfavorable pressure gradients over the airfoil. The effect is magnified as the Reynolds number decreases.

Although the rather high value of the minimum drag shown by the NACA 23012 and NACA 23015 airfoil sections (figs. 5 and 6) precludes the possibility of very extensive laminar boundary layers on the airfoil surfaces, the jog near zero lift which appears in all of the drag polars for these sections suggests the formation of laminar boundary layers. Theoretical calculations of the pressure distribution around the NACA 23012 and NACA 23015 airfoil sections indicate that the pressure gradients over the lower surfaces become favorable to laminar flow at lift coefficients above a small positive value. The jog in the drag polar near zero lift corresponds, therefore, to the formation of laminar layers on the lower surface. At the higher lift coefficients, the manner in which the drag increases above the flat portion of the polar depends markedly on the Reynolds number. Between Reynolds numbers of 9.0×10^6 and 3.0×10^6 the drag rises gradually. At the lower Reynolds numbers, the drag rise is preceded by a jog which increases in intensity and occurs at progressively lower lift coefficients as the Reynolds number is reduced. Although boundary-layer surveys were not made, the behavior of this jog as the Reynolds number is lowered suggests the formation of a laminar separation bubble near the leading edge of the upper surface.

The drag polars for the airfoils with roughened leading edges do not have a range of lift coefficients over which the drag is essentially constant, but rather, are of parabolic form. The lower portion of the parabolas, over which the drag variation with lift coefficient is least, appears to become narrower for all the airfoils as the Reynolds number

is reduced, except at the lowest Reynolds number (0.7×10^6). The behavior of the drag polars at a Reynolds number of 0.7×10^6 probably results from the fact that the leading-edge roughness employed was not sufficiently large to cause fully developed turbulent boundary layers at this low value of the Reynolds number. In the rough condition, airfoil-thickness ratio does not appear to have a very pronounced effect upon the lift-coefficient range corresponding to the lower portion of the drag polar, nor is there very much difference in this range for the NACA 23012 and NACA 23015 airfoils as compared to the NACA 64-series sections.

The Reynolds number has a very important effect upon the minimum drag (figs. 1 to 6) of the airfoils, both in the smooth condition and with rough leading edges. In order to show more clearly the magnitude of this trend, the drag coefficient corresponding to the design lift coefficient has been plotted in figure 7 as a function of Reynolds number for each of the six airfoils tested. The minimum-drag coefficient is seen to increase with decreasing Reynolds number for all the airfoils, both smooth and rough, but the magnitude of the effect seems to be greatest when the leading edges of the airfoils are in the rough condition. The previously mentioned effect of roughness size is probably responsible for the drag reduction shown by the results for the rough airfoils at a Reynolds number of 0.7×10^6 . The amount by which the minimum drag increases as the Reynolds number is lowered appears to become larger as the thickness ratio of the smooth NACA 64-series sections increases. The results for the two NACA 230-series airfoils do not appear to follow this trend. On the basis of these limited data then, the advantage of using an NACA 64-series airfoil becomes less as the Reynolds number is lowered and the airfoil-thickness ratio is increased. In the rough condition, there is little difference in the minimum drag of the NACA 64-series and NACA 230-series airfoils.

Lift.— The lift parameters which are usually considered to be the most important are the lift-curve slope, the angle of zero lift, and the maximum lift coefficient. From the lift data presented in figures 1 to 6, the values of these parameters have been determined at each Reynolds number for the six airfoils tested, and are plotted as a function of Reynolds number in figures 8 to 10.

According to reference 1, the lift-curve slope is defined as the slope of the lift curve as it passes through the design lift coefficient. Because the low dynamic pressures necessary in the present investigation reduced the accuracy of the measuring apparatus, some scatter is present in the lift data. For this reason and because some of the lift curves had slight jogs near the design lift coefficient at the lower Reynolds numbers, comparable measurements of the lift-curve slope for different Reynolds numbers did not appear possible by the method of reference 1. The lift-curve slopes of the airfoils tested in this investigation were therefore considered to be defined by the best straight line through the data between zero-lift and the design lift coefficient. The slopes corresponding to all the Reynolds numbers from 9.0×10^6 to 0.7×10^6

were measured according to this procedure and are presented in figure 8 as a function of Reynolds number. Some decreases in lift-curve slope are seen to accompany a decrease in Reynolds number for all the smooth airfoils except the NACA 64₃-418. The lift-curve slope of this particular section seems to be nearly independent of Reynolds number. The magnitude of the scale effect on the lift-curve slope increases somewhat, particularly for the NACA 23012 and NACA 23015, when the airfoil leading edges are rough.

Although the angles of zero lift shown in figure 9 for the six airfoils do increase somewhat in a negative direction as the Reynolds number is lowered, the magnitude of the effect does not appear to be significant.

The lift parameter which is most affected by variations in the Reynolds number is the maximum lift coefficient. In all cases, decreasing the Reynolds number from 9.0×10^6 to 0.7×10^6 causes a reduction in the maximum lift of the airfoils (fig. 10) both in the smooth condition and with rough leading edges. The manner in which the maximum lift of the airfoils, both smooth and rough, varies with Reynolds number and the magnitude of this variation depend upon the airfoil design and upon the use of a split flap. A sufficient amount of data is not available to permit the formulation of detailed conclusions regarding the effect of these parameters upon the manner in which the maximum lift varies with Reynolds number. One important general conclusion, however, is evident from a study of the data presented in figure 10. A consideration of these data indicates that the comparative merits of a group of airfoils based on data for a particular Reynolds number and surface condition may change radically as the surface condition and Reynolds number are varied.

Consider, for example, the manner in which the comparative values of the maximum lift of the NACA 64-409 and NACA 64₁-412 change as the Reynolds number is lowered from 9.0×10^6 to 0.7×10^6 . Notice also that the rather large advantage of the NACA 23012 as compared to the NACA 64₁-412 decreases and finally vanishes as the Reynolds number is progressively reduced from 9.0×10^6 to 0.7×10^6 . The effect of surface roughness upon the comparison of the airfoils is quite pronounced. For example, in the rough condition, the maximum lift of the NACA 23012 becomes progressively less than that of the NACA 64₁-412 as the Reynolds number is reduced and is actually less than that of the NACA 64-409 below 2.0×10^6 . Also of interest is the fact that the decrement in maximum lift due to roughness decreases and finally disappears as the Reynolds number of the thinner NACA 6-series sections is lowered to 0.7×10^6 , while a rather large decrease in the maximum lift of the NACA 230-series sections is caused by roughness, even at this low value of the Reynolds number. With split flaps deflected 60° , the data of figure 10 show that the amount and type of maximum-lift variation with Reynolds number are not necessarily the same as indicated by the results for the plain airfoils; and again, the comparative values of the maximum

lift for the various airfoils with split flaps are seen to change with the Reynolds number and surface condition.

Pitching moment and aerodynamic center.- The value of the quarter-chord pitching-moment coefficient corresponding to the design angle of attack shows practically no variation with Reynolds number (figs. 1 to 6). Accompanying changes in the Reynolds number, some change in the variation of the moment coefficient with angle of attack is noticeable. Consequently, the chordwise position of the aerodynamic center varies somewhat with Reynolds number. These variations, however, do not appear to form any consistent trend as the airfoil thickness and Reynolds number are varied.

CONCLUSIONS

From an investigation of the two-dimensional aerodynamic characteristics of four NACA 64-series and two NACA 230-series airfoil sections at Reynolds numbers from 9.0×10^6 to 0.7×10^6 , the following conclusions may be drawn:

1. The minimum drag of each of the smooth airfoils increased progressively as the Reynolds number was lowered from 9.0×10^6 to 0.7×10^6 . The magnitude of this increase appeared to become larger as the thickness ratio of the NACA 64-series sections was increased.

2. Decreasing the Reynolds number from 9.0×10^6 to 0.7×10^6 caused a reduction in the maximum lift of all the airfoils both in the smooth and rough condition. The magnitude and character of this reduction, however, varied with airfoil design and surface condition so that the comparative merits of the various airfoils changed markedly with Reynolds number and surface condition.

3. Although the results are not entirely consistent, some decreases in the lift-curve slope of both the smooth and rough airfoils usually accompanied a reduction in Reynolds number.

4. Both the angle of zero lift and the quarter-chord pitching moment appeared to be nearly independent of variations in the Reynolds number between 9.0×10^6 and 0.7×10^6 .

Langley Memorial Aeronautical Laboratory
National Advisory Committee for Aeronautics
Langley Field, Va.

REFERENCES

1. Abbott, Ira H., von Doenhoff, Albert E., and Stivers, Louis S., Jr.:
Summary of Airfoil Data. NACA ACR No. L5C05, 1945.
2. von Doenhoff, Albert E., and Abbott, Frank T., Jr.: The Langley Two-
Dimensional Low-Turbulence Pressure Tunnel. NACA TN No. 1283, 1947.

TABLE I
ORDINATES OF NACA AIRFOIL SECTIONS TESTED

NACA 64-409

[Stations and ordinates given in percent of airfoil chord]

Upper surface		Lower surface	
Station	Ordinate	Station	Ordinate
0	0	0	0
.377	.829	.623	-.629
.613	1.021	.887	-.741
1.095	1.331	1.405	-.903
2.322	1.895	2.678	-1.151
4.803	2.732	5.197	-1.468
7.297	3.383	7.703	-1.687
9.798	3.925	10.202	-1.857
14.810	4.796	15.190	-2.104
19.830	5.456	20.170	-2.272
24.854	5.957	25.146	-2.377
29.882	6.315	30.118	-2.427
34.912	6.538	35.088	-2.418
39.942	6.632	40.058	-2.348
44.972	6.554	45.028	-2.174
50.000	6.342	50.000	-1.930
55.024	6.016	54.976	-1.636
60.045	5.594	59.955	-1.310
65.060	5.085	64.940	-.965
70.069	4.504	69.931	-.616
75.072	3.858	74.928	-.278
80.069	3.154	79.931	.030
85.059	2.413	84.941	.279
90.043	1.644	89.957	.424
95.021	.858	94.979	.406
100.000	0	100.000	0

L.E. radius: 0.579

Slope of radius through L.E.: 0.168

NACA 641-412

[Stations and ordinates given in percent of airfoil chord]

Upper surface		Lower surface	
Station	Ordinate	Station	Ordinate
0	0	0	0
.338	1.004	.662	-.864
.569	1.305	.931	-1.025
1.045	1.690	1.455	-1.262
2.264	2.393	2.736	-1.649
4.738	3.430	5.262	-2.166
7.229	4.231	7.771	-2.535
9.730	4.896	10.270	-2.828
14.745	5.959	15.255	-3.267
19.772	6.760	20.228	-3.576
24.805	7.363	25.195	-3.783
29.842	7.786	30.158	-3.898
34.882	8.037	35.118	-3.917
39.923	8.123	40.077	-3.839
44.963	7.988	45.037	-3.608
50.000	7.686	50.000	-3.274
55.032	7.246	54.968	-2.866
60.059	6.690	59.941	-2.406
65.078	6.033	64.922	-1.913
70.090	5.293	69.910	-1.405
75.094	4.483	74.906	-.903
80.089	3.619	79.911	-.435
85.076	2.722	84.924	-.038
90.055	1.818	89.945	.250
95.027	.919	94.973	.345
100.000	0	100.000	0

L.E. radius: 1.040

Slope of radius through L.E.: 0.168



NACA 642-415

[Stations and ordinates given in percent of airfoil chord]

Upper surface		Lower surface	
Station	Ordinate	Station	Ordinate
0	0	0	0
.299	1.291	.701	-1.091
.524	1.579	.974	-1.299
.996	2.038	1.504	-1.610
2.207	2.883	2.793	-2.139
4.673	4.121	5.327	-2.857
7.162	5.075	7.838	-3.379
9.662	5.864	10.338	-3.796
14.681	7.122	15.319	-4.430
19.714	8.066	20.286	-4.882
24.756	8.771	25.244	-5.191
29.803	9.260	30.197	-5.372
34.853	9.541	35.147	-5.421
39.904	9.614	40.096	-5.330
44.954	9.414	45.046	-5.034
50.000	9.016	50.000	-4.604
55.040	8.456	54.960	-4.076
60.072	7.762	59.928	-3.478
65.096	6.954	64.894	-2.834
70.111	6.059	69.889	-2.167
75.115	5.084	74.885	-1.504
80.109	4.062	79.891	-.878
85.092	3.020	84.908	-.328
90.066	1.982	89.924	.086
95.032	.976	94.968	.288
100.000	0	100.000	0

L.E. radius: 1.590

Slope of radius through L.E.: 0.168

NACA 643-418

[Stations and ordinates given in percent of airfoil chord]

Upper surface		Lower surface	
Station	Ordinate	Station	Ordinate
0	0	0	0
.263	1.508	.737	-1.308
.486	1.840	1.014	-1.560
.950	2.370	1.550	-1.942
2.152	3.557	2.848	-2.613
4.609	4.800	5.391	-3.536
7.095	5.908	7.905	-4.212
9.595	6.823	10.405	-4.755
14.617	8.277	15.383	-5.485
19.657	9.366	20.343	-6.182
24.707	10.176	25.293	-6.596
29.763	10.730	30.237	-6.842
34.823	11.037	35.177	-6.917
39.885	11.093	40.115	-6.809
44.945	10.820	45.055	-6.440
50.000	10.320	50.000	-5.908
55.047	9.635	54.953	-5.255
60.086	8.799	59.914	-4.515
65.114	7.841	64.886	-3.721
70.131	6.784	69.869	-2.896
75.135	5.654	74.865	-2.074
80.127	4.477	79.873	-1.293
85.108	3.264	84.892	-.602
90.077	2.132	89.923	-.064
95.037	1.030	94.963	.234
100.000	0	100.000	0

L.E. radius: 2.208

Slope of radius through L.E.: 0.168

TABLE I
ORDINATES OF NACA AIRFOIL SECTIONS TESTED -
Concluded

NACA 23012

[Stations and ordinates given in
percent of airfoil chord]

Upper surface		Lower surface	
Station	Ordinate	Station	Ordinate
0	----	0	0
1.25	2.67	1.25	-1.23
2.5	3.61	2.5	-1.71
5.0	4.91	5.0	-2.26
7.5	5.80	7.5	-2.61
10	6.43	10	-2.92
15	7.19	15	-3.50
20	7.50	20	-3.97
25	7.60	25	-4.28
30	7.55	30	-4.46
40	7.14	40	-4.48
50	6.41	50	-4.17
60	5.47	60	-3.67
70	4.36	70	-3.00
80	3.08	80	-2.16
90	1.68	90	-1.23
95	.92	95	-.70
100	(.13)	100	(-.13)
100	----	100	0

L.E. radius: 1.58
Slope of radius through L.E.: 0.305

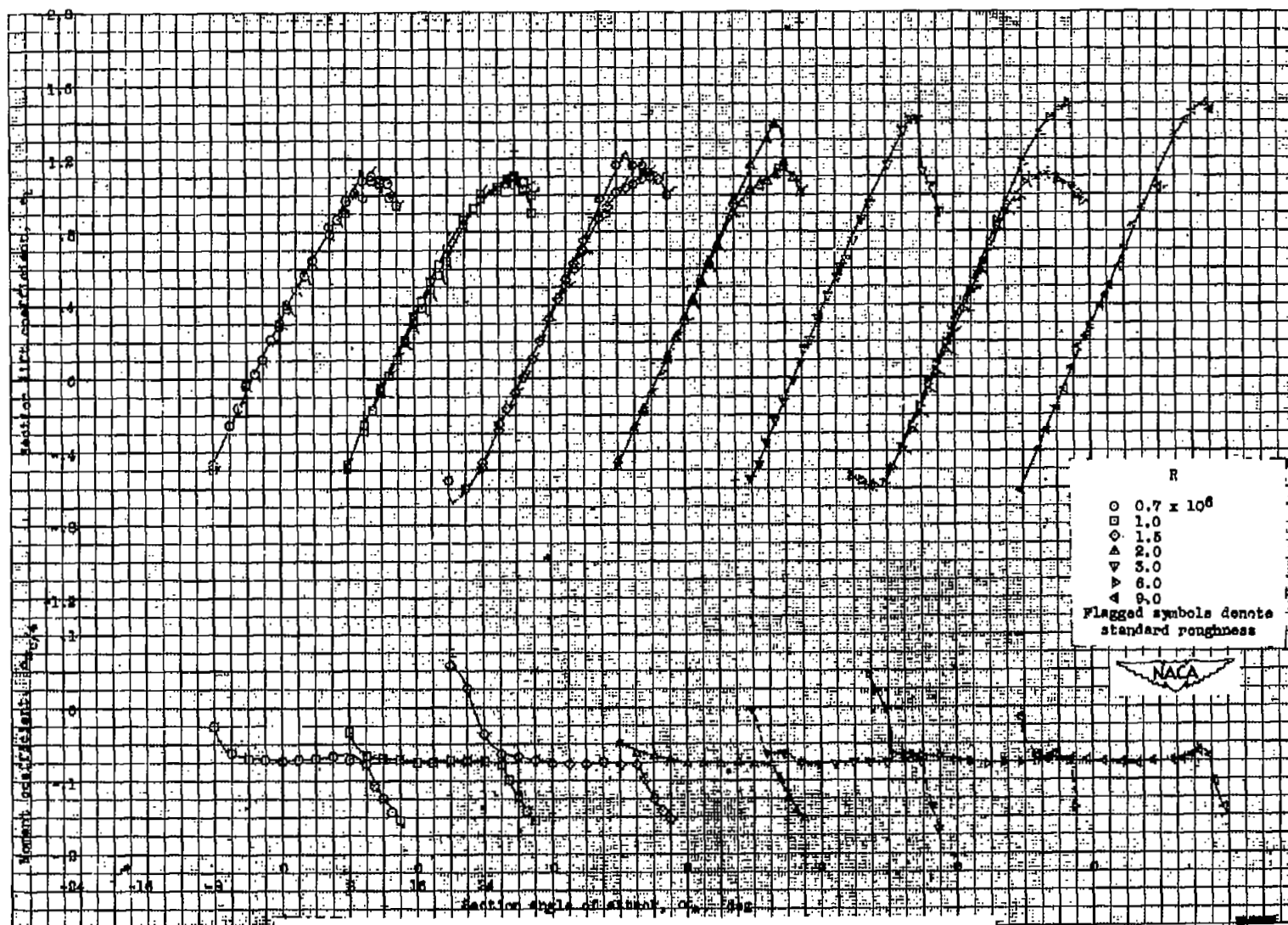


NACA 23015

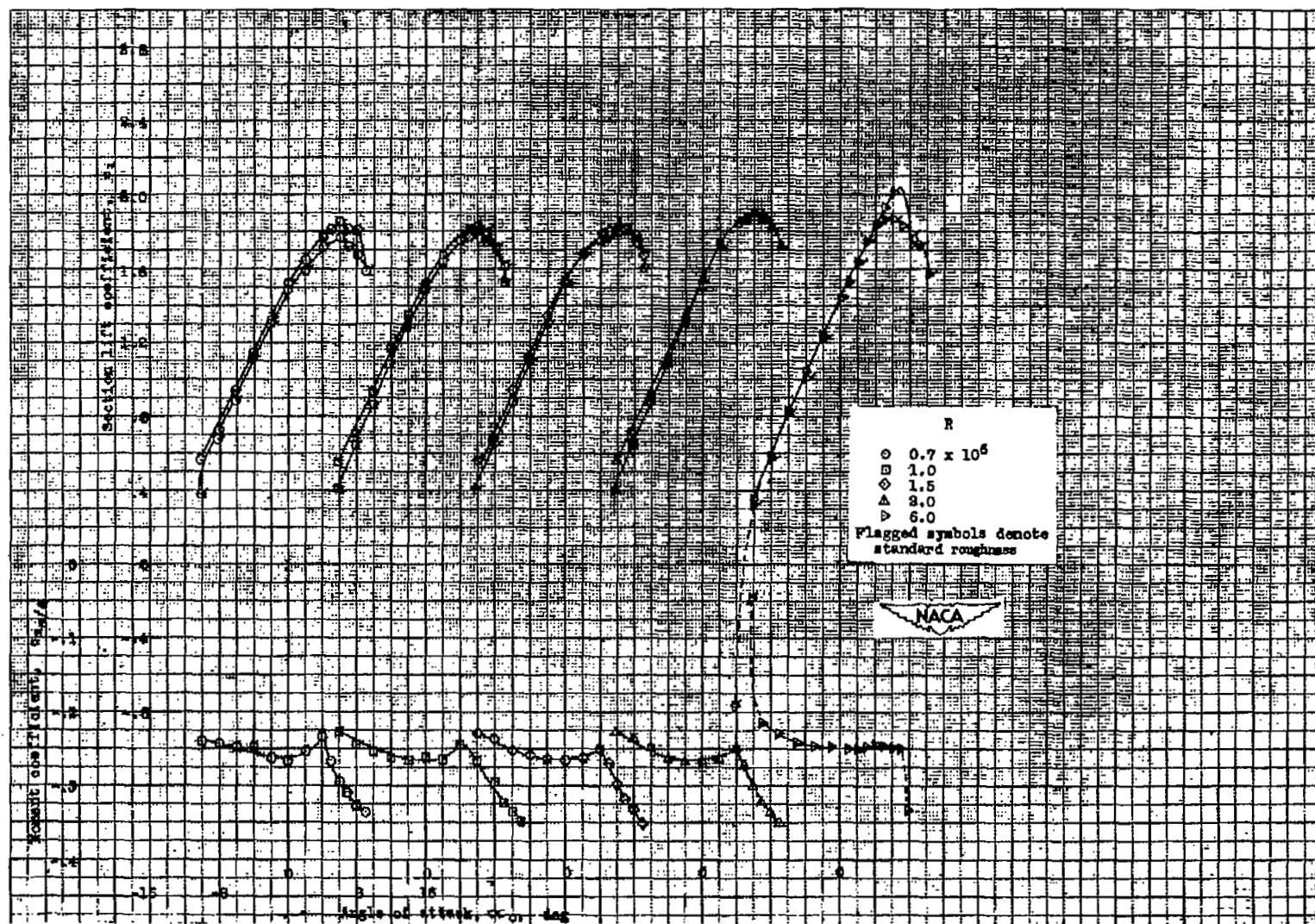
[Stations and ordinates given in
percent of airfoil chord]

Upper surface		Lower surface	
Station	Ordinate	Station	Ordinate
0	----	0	0
1.25	3.34	1.25	-1.54
2.5	4.44	2.5	-2.25
5.0	5.89	5.0	-3.04
7.5	6.91	7.5	-3.61
10	7.64	10	-4.09
15	8.52	15	-4.84
20	8.92	20	-5.41
25	9.08	25	-5.78
30	9.05	30	-5.96
40	8.59	40	-5.92
50	7.74	50	-5.50
60	6.61	60	-4.81
70	5.25	70	-3.91
80	3.73	80	-2.83
90	2.04	90	-1.59
95	1.12	95	-.90
100	(.16)	100	(-.16)
100	----	100	0

L.E. radius: 2.48
Slope of radius through L.E.: 0.305

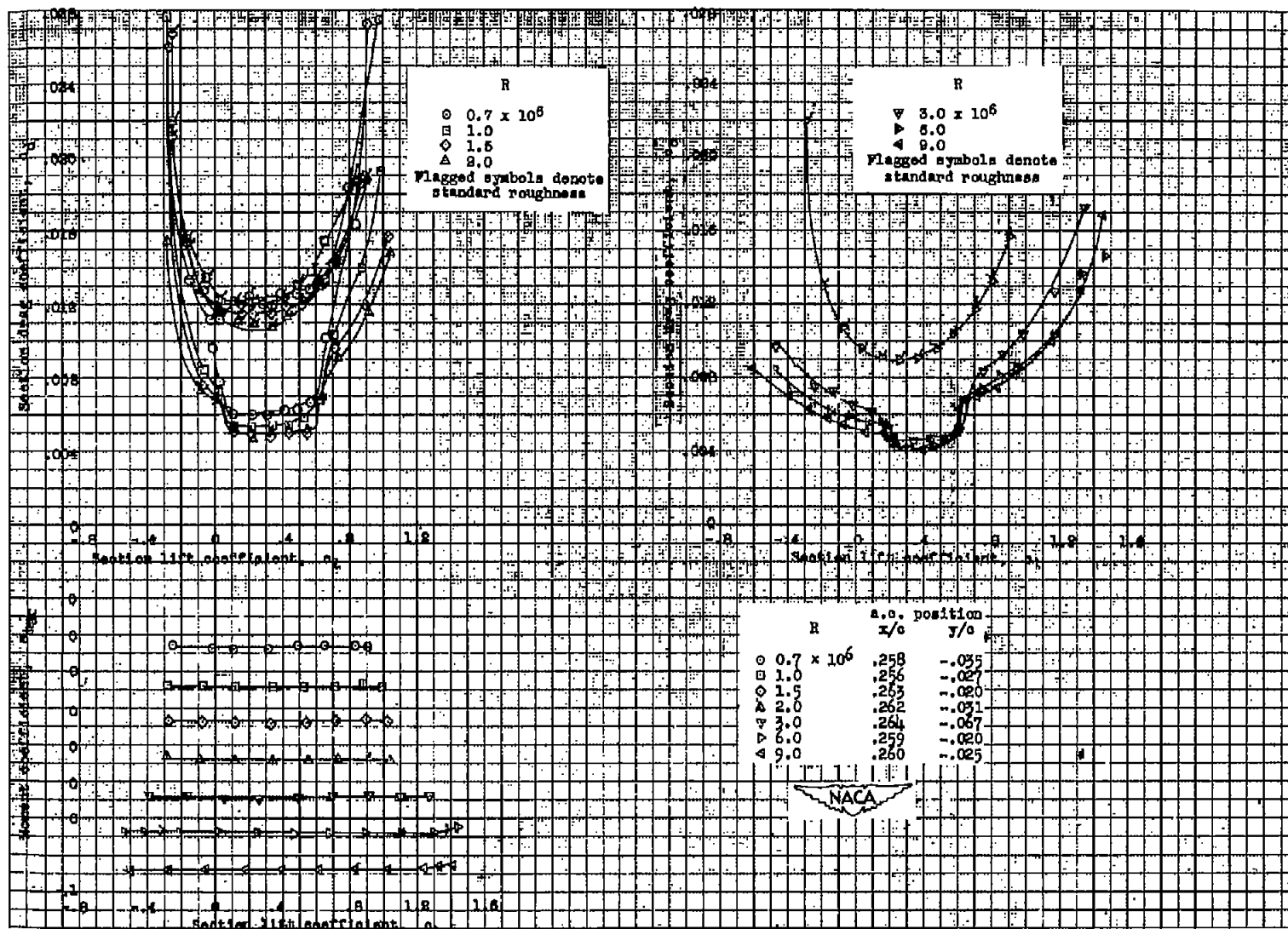


(a) Section lift and pitching-moment characteristics of the plain airfoil section.
 Figure 1. Aerodynamic characteristics of the NACA 64-409 Airfoil section, 24-inch chord. Tests, TDT 995, and LTT 458.



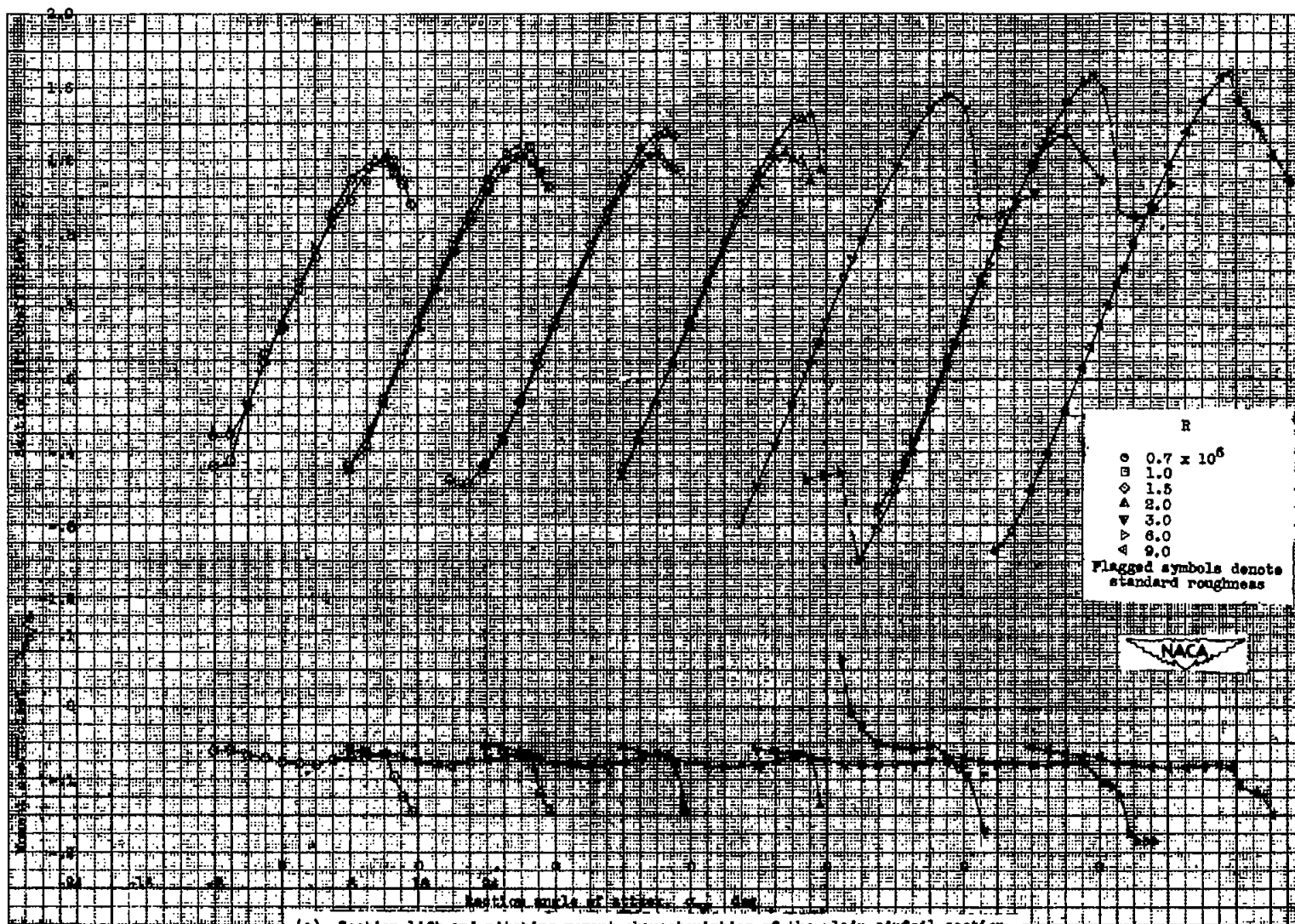
(b) Section lift and pitching-moment characteristics of the NACA 64-409 airfoil section with a 0.20c simulated split flap deflected 60°.

Figure 1.- Continued.



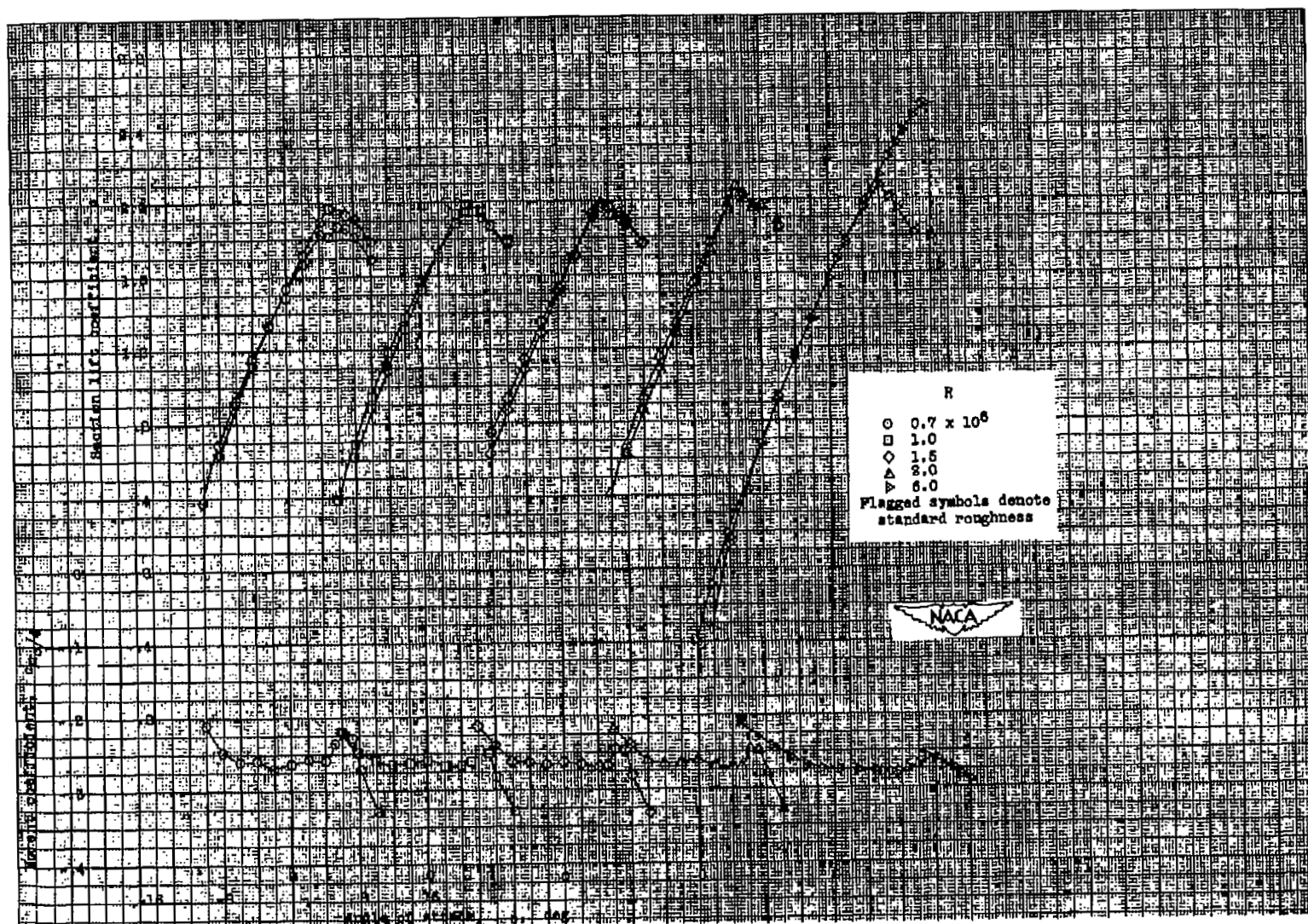
(a) Section drag characteristics and section pitching-moment characteristics about the aerodynamic center of the plain NACA 64-109 airfoil section.

Figure 1.- Concluded.



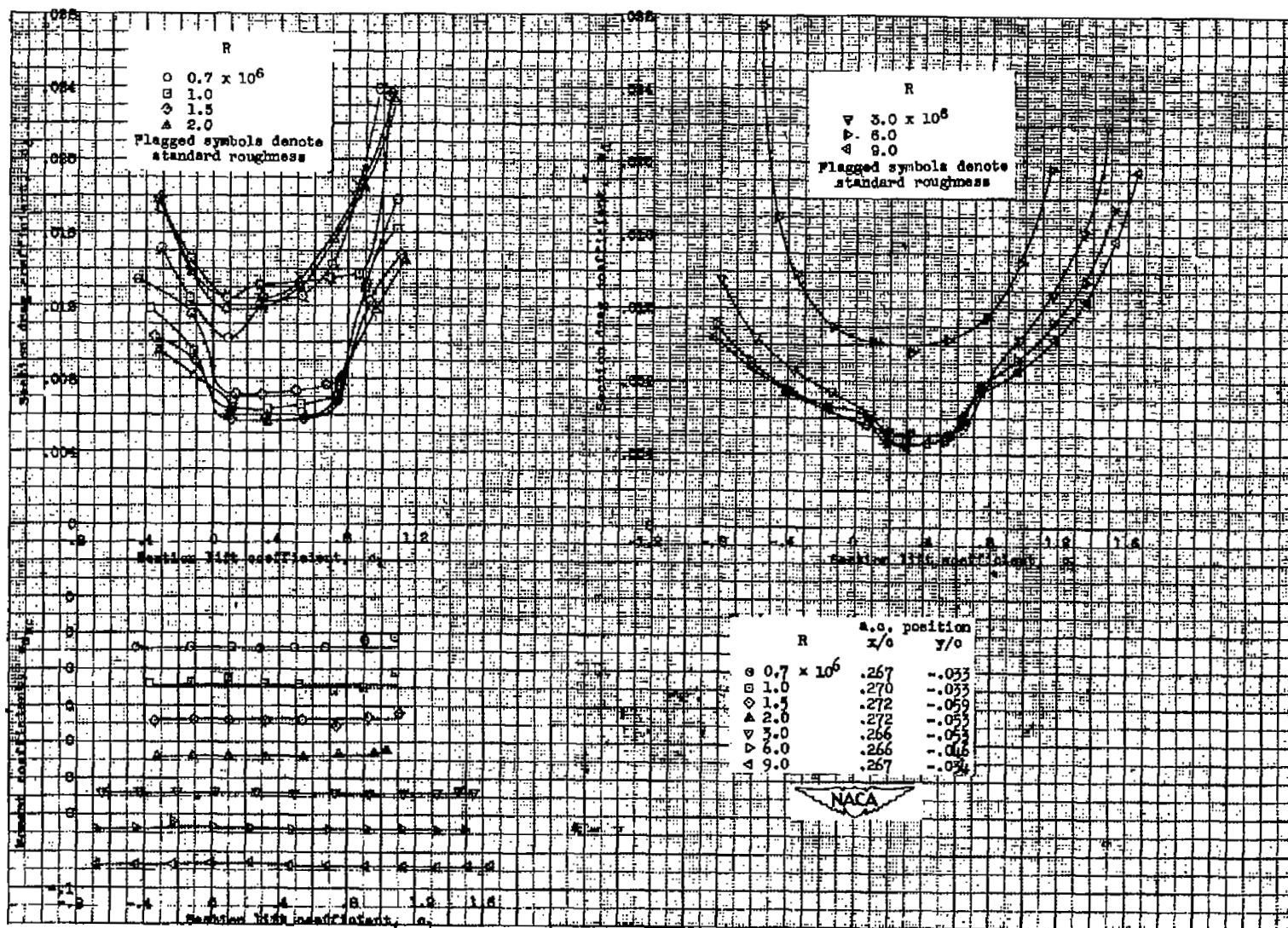
(a) Section lift and pitching-moment characteristics of the plain airfoil section.

Figure 2.- Aerodynamic characteristics of the NACA 64₁-412 airfoil section, 24-inch chord. Tests, TDT 682, 686, 831, and IRT 447.



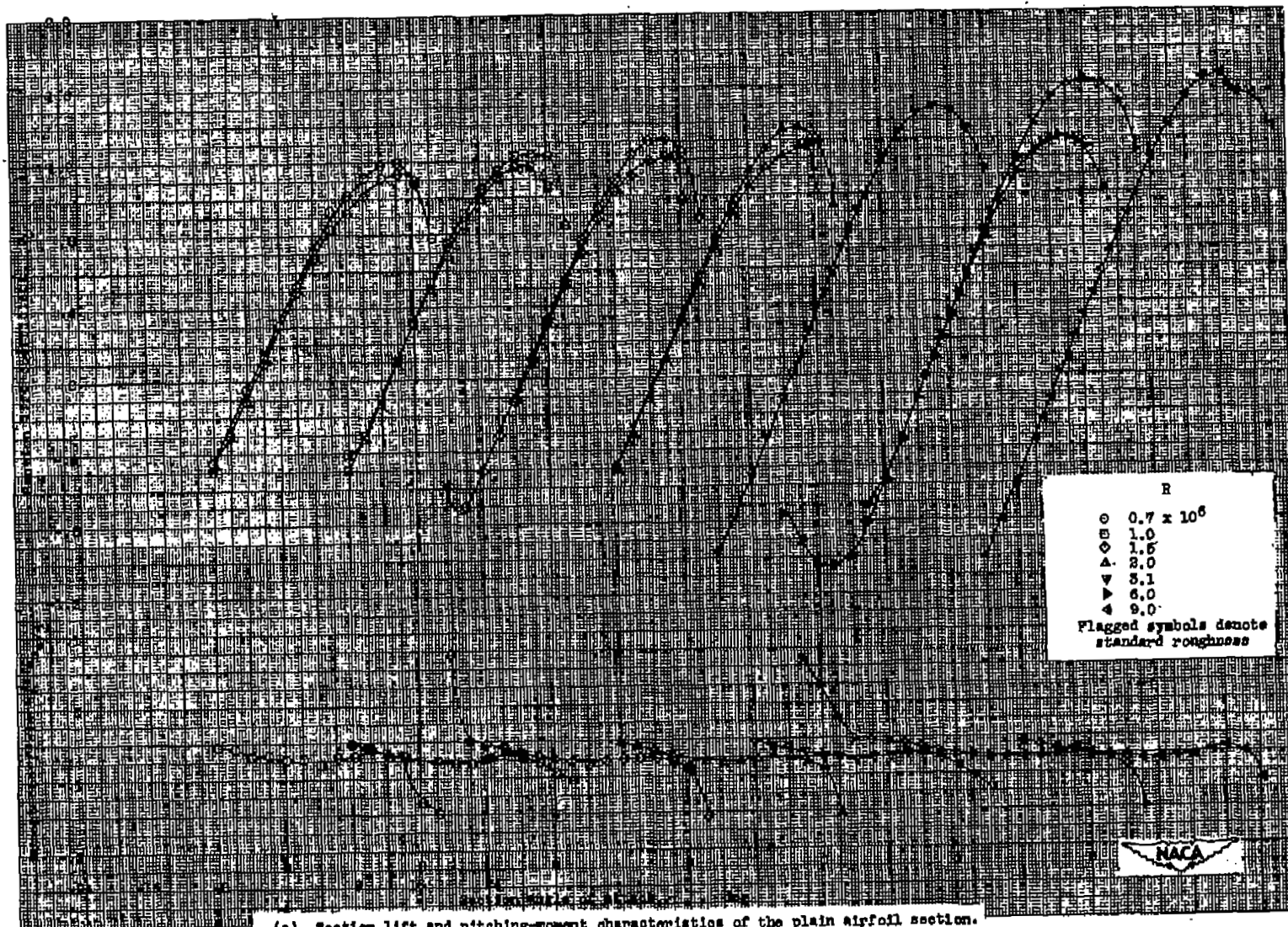
(b) Section lift and pitching-moment characteristics of the NACA 64₁-412 airfoil section with a 0.20c simulated split flap deflected 60°.

Figure 2.- Continued.



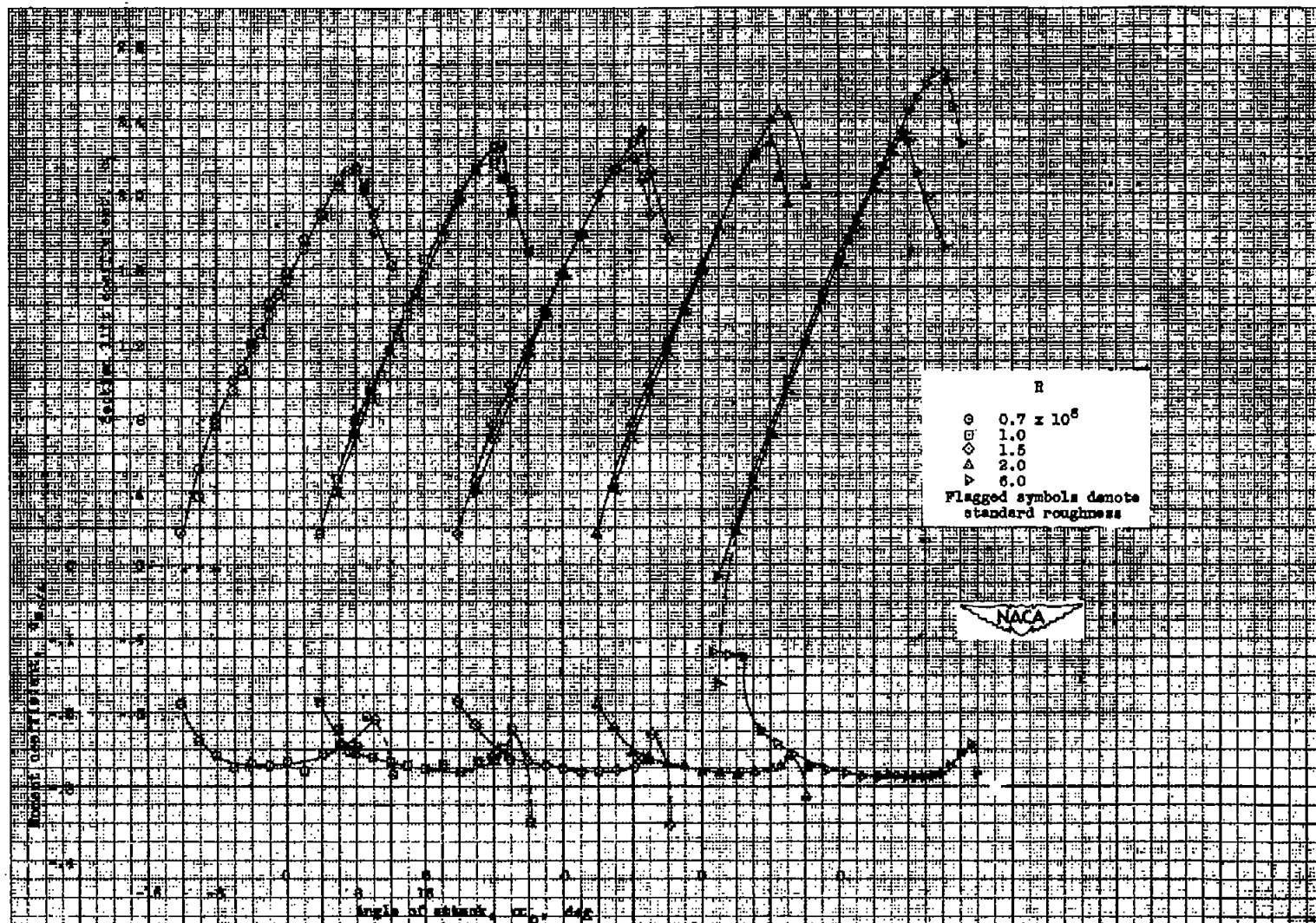
(c) Section drag characteristics and section pitching-moment characteristics about the aerodynamic center of the plain NACA 64-112 airfoil section.

Figure 2.- Concluded.



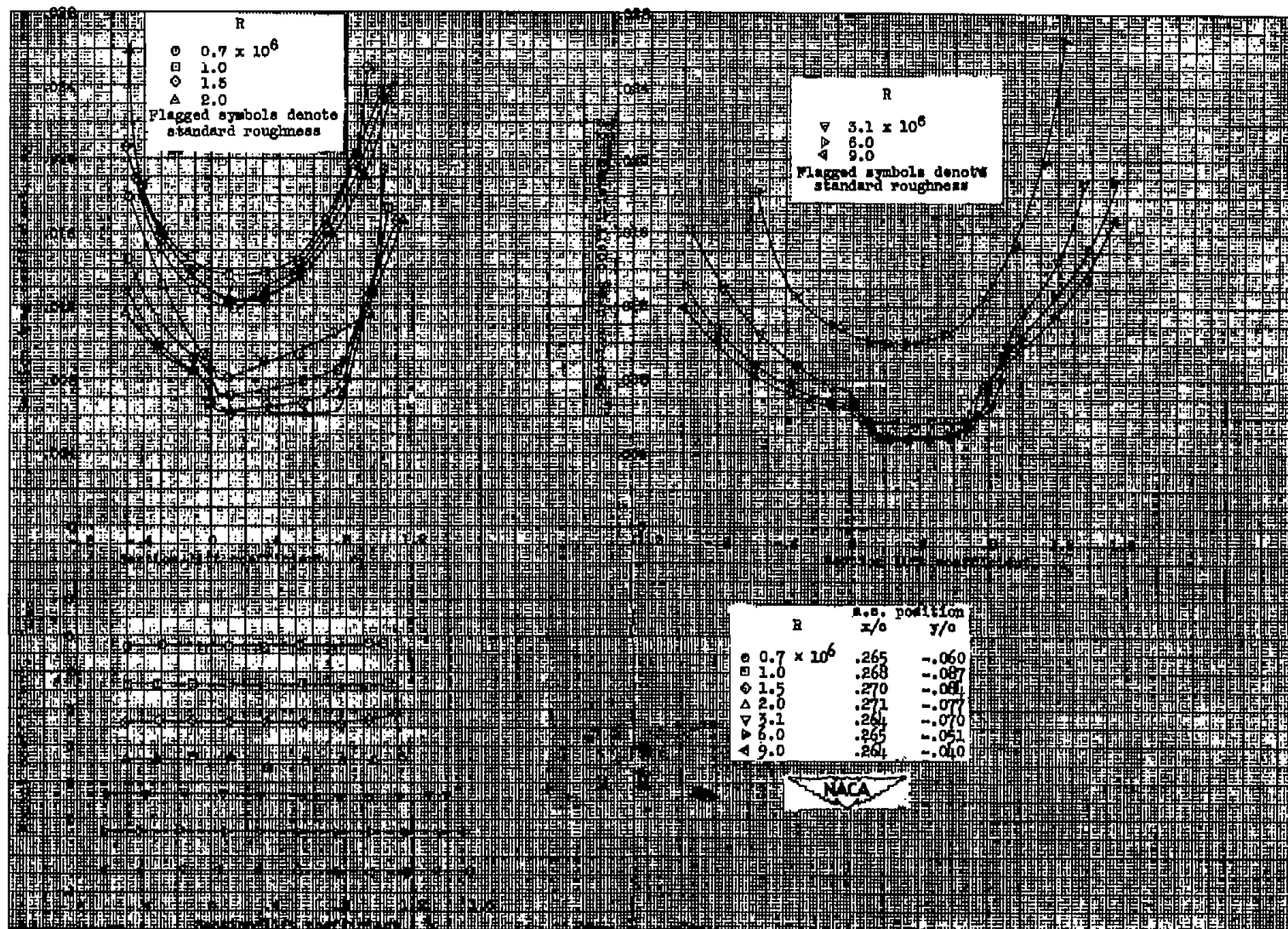
(a) Section lift and pitching-moment characteristics of the plain airfoil section.

Figure 3.- Aerodynamic characteristics of the NACA 64_g-415 airfoil section, 24-inch chord. Tests, TDT 656, 685, 735, and LPT 446.



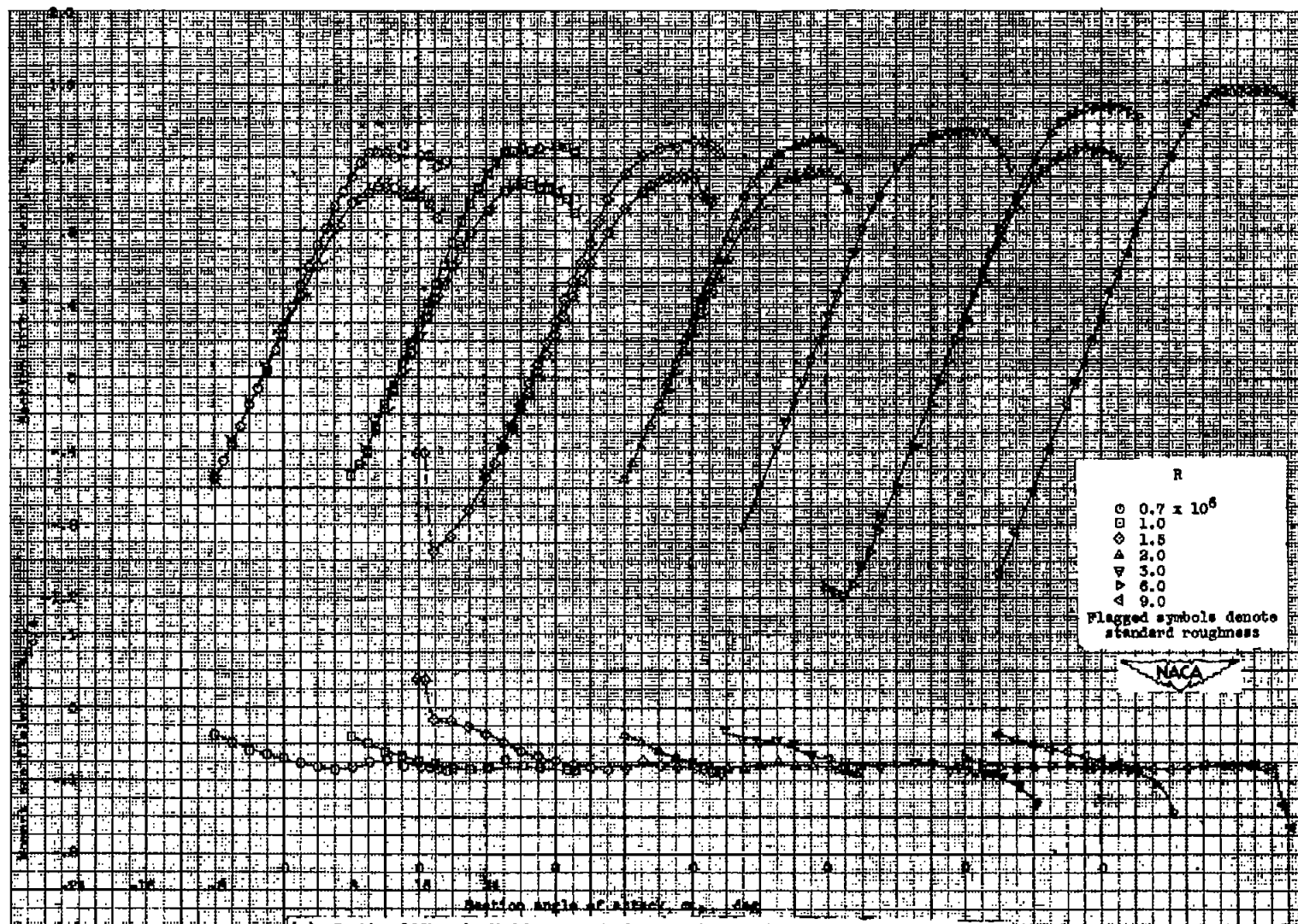
(b) Section lift and pitching-moment characteristics of the NACA G₂-415 airfoil section with a 0.20c simulated split flap deflected 60°.

Figure 3.- Continued.



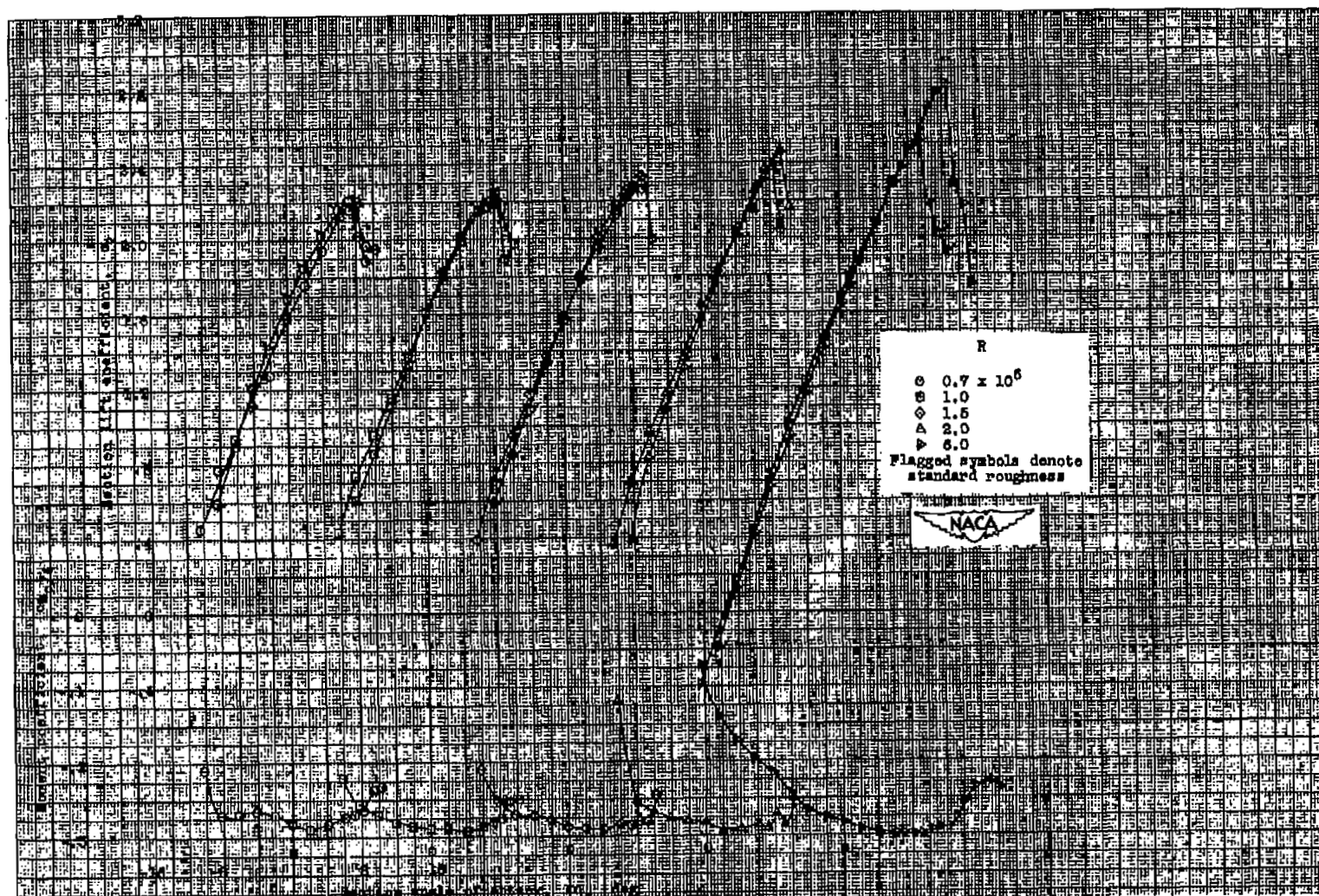
(c) Section drag characteristics and section pitching-moment characteristics about the aerodynamic center of the plain NACA 642-415 airfoil section.

Figure 3.- Concluded.



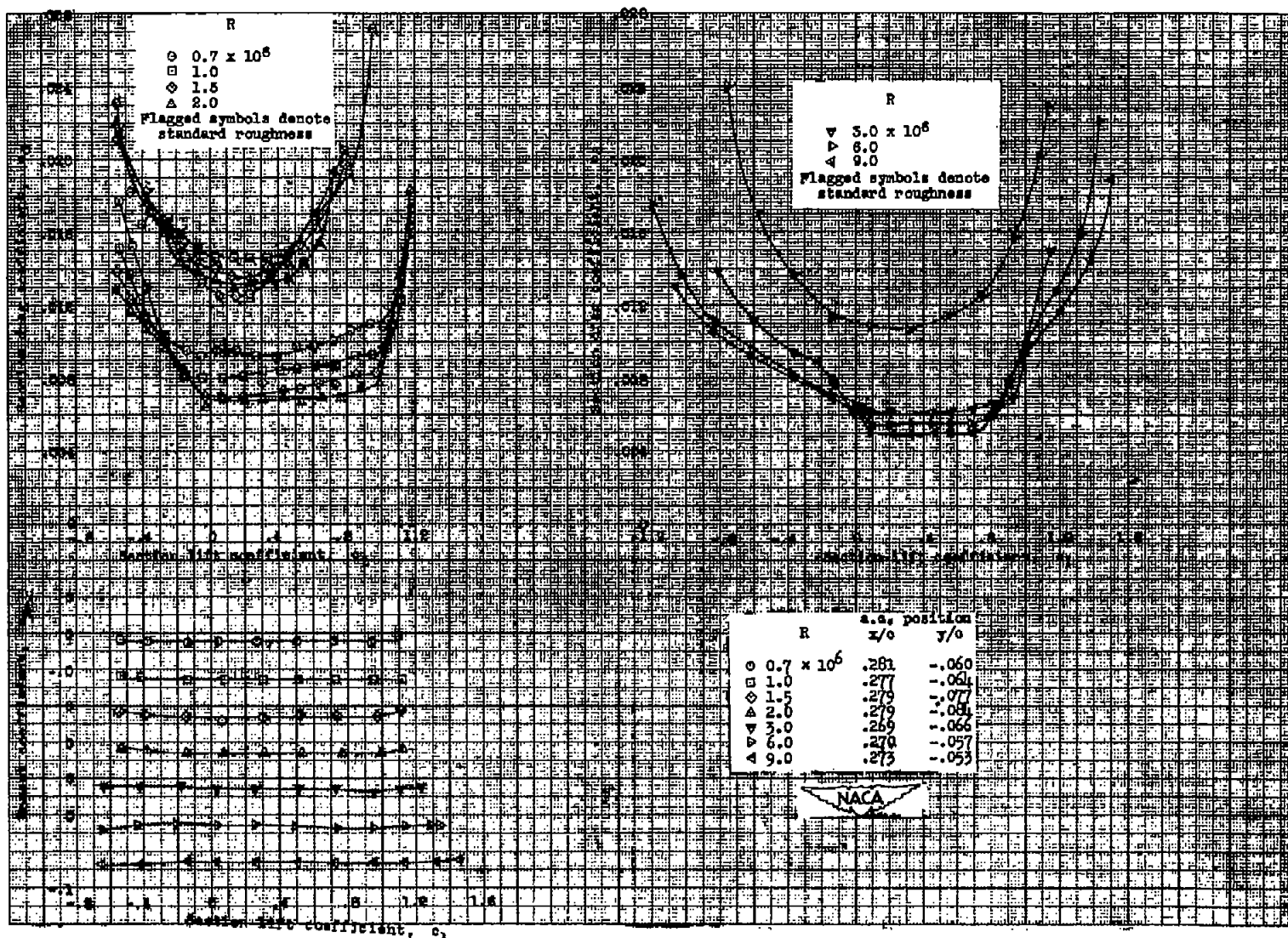
(a) Section lift and pitching-moment characteristics of the plain airfoil section.

Figure 4.- Aerodynamic characteristics of the NACA 64-418 airfoil section, 24-inch chord. Tests, TDT 735, 736, and LTT 450.



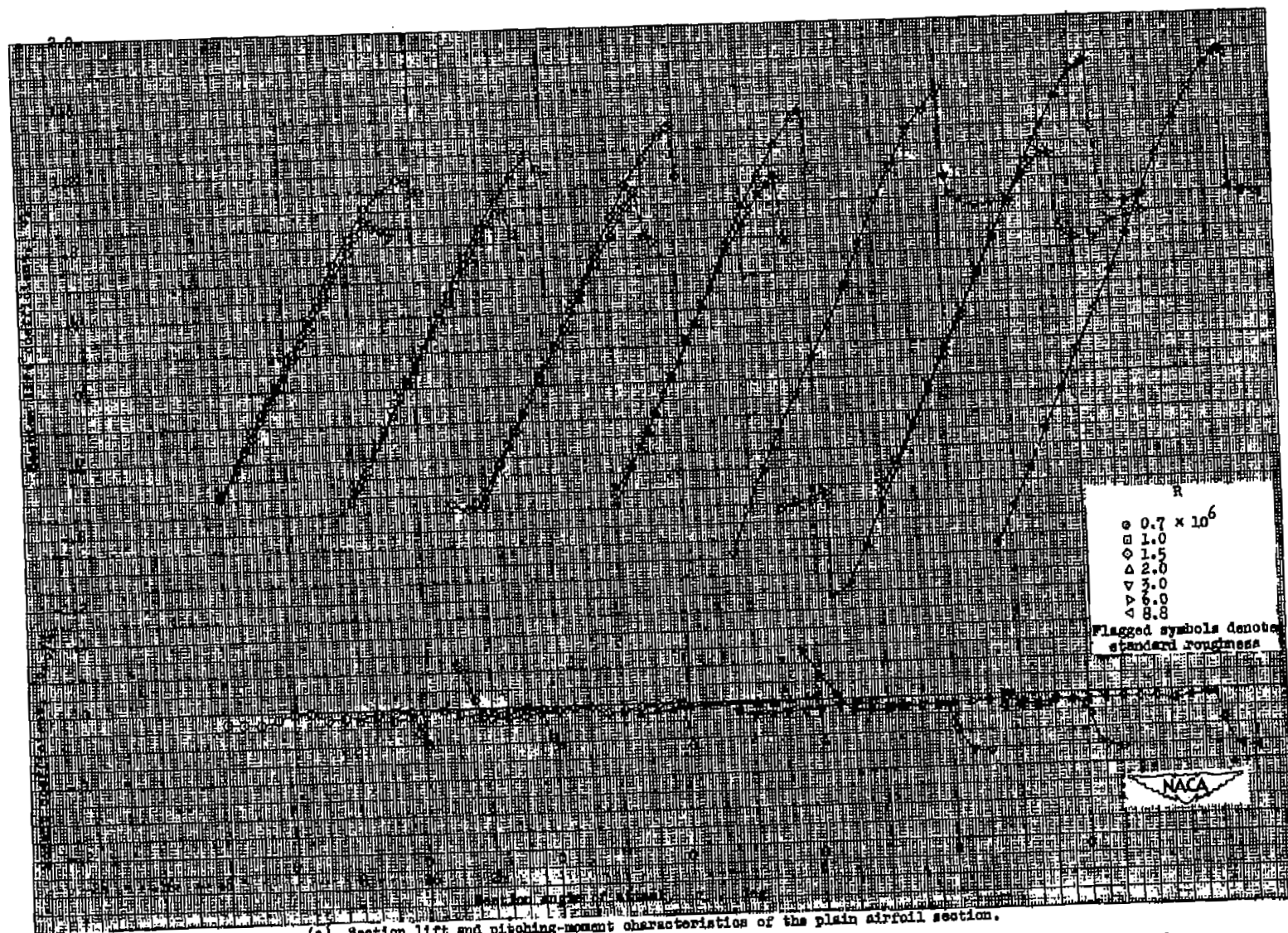
(b) Section lift and pitching-moment characteristics of the NACA 64-418 airfoil section with a 0.20c simulated split flap deflected 60°.

Figure 4.- Continued.



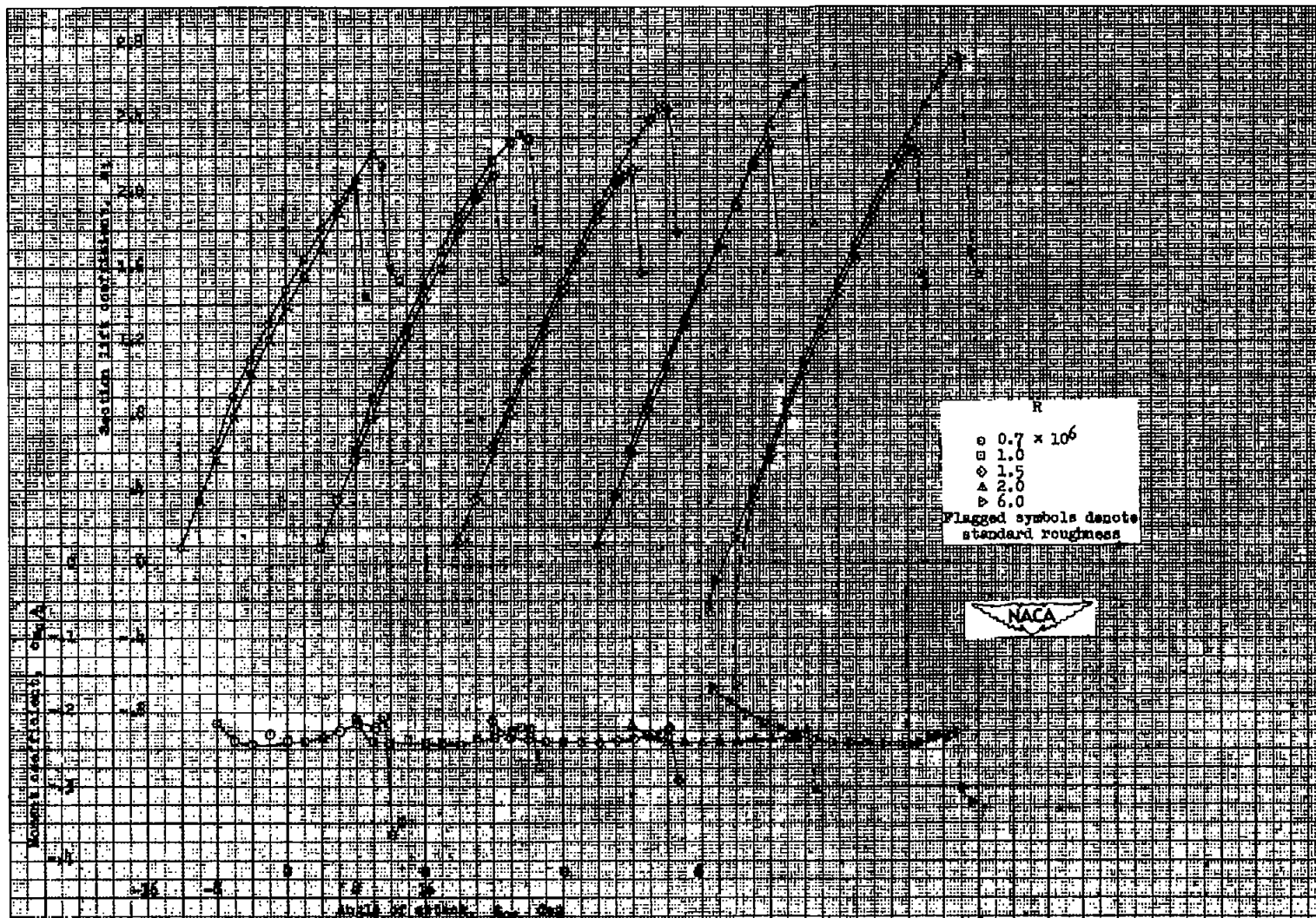
(c) Section drag characteristics and section pitching-moment characteristics about the aerodynamic center of the plain NACA 64-18 airfoil section.

Figure 4.- Concluded.



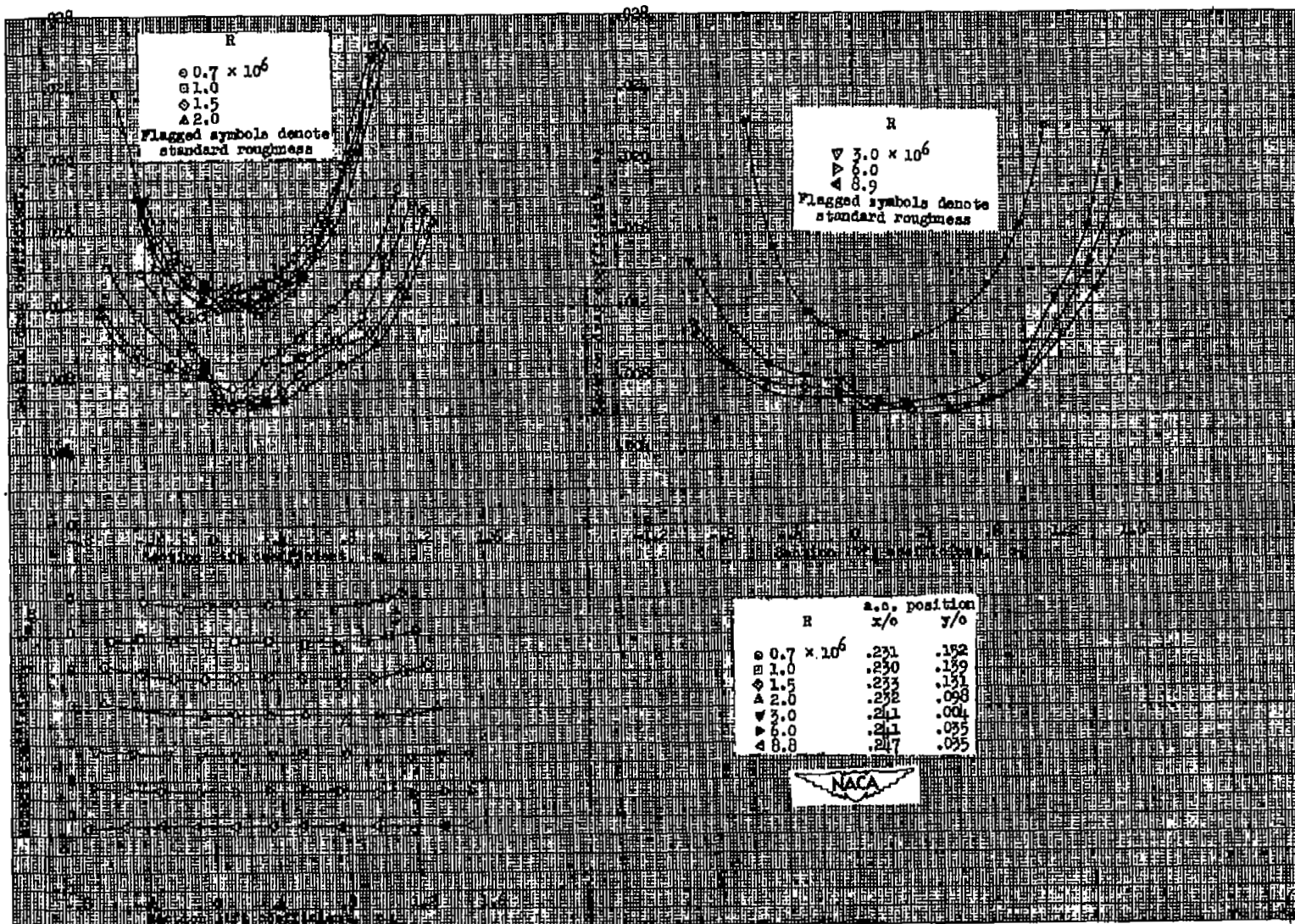
(a) Section lift and pitching-moment characteristics of the plain airfoil section.

Figure 5-- Aerodynamic characteristics of the NACA 23012 airfoil section, 24-inch chord. Tests, NTF 494, 497, 523, and NTF 451.



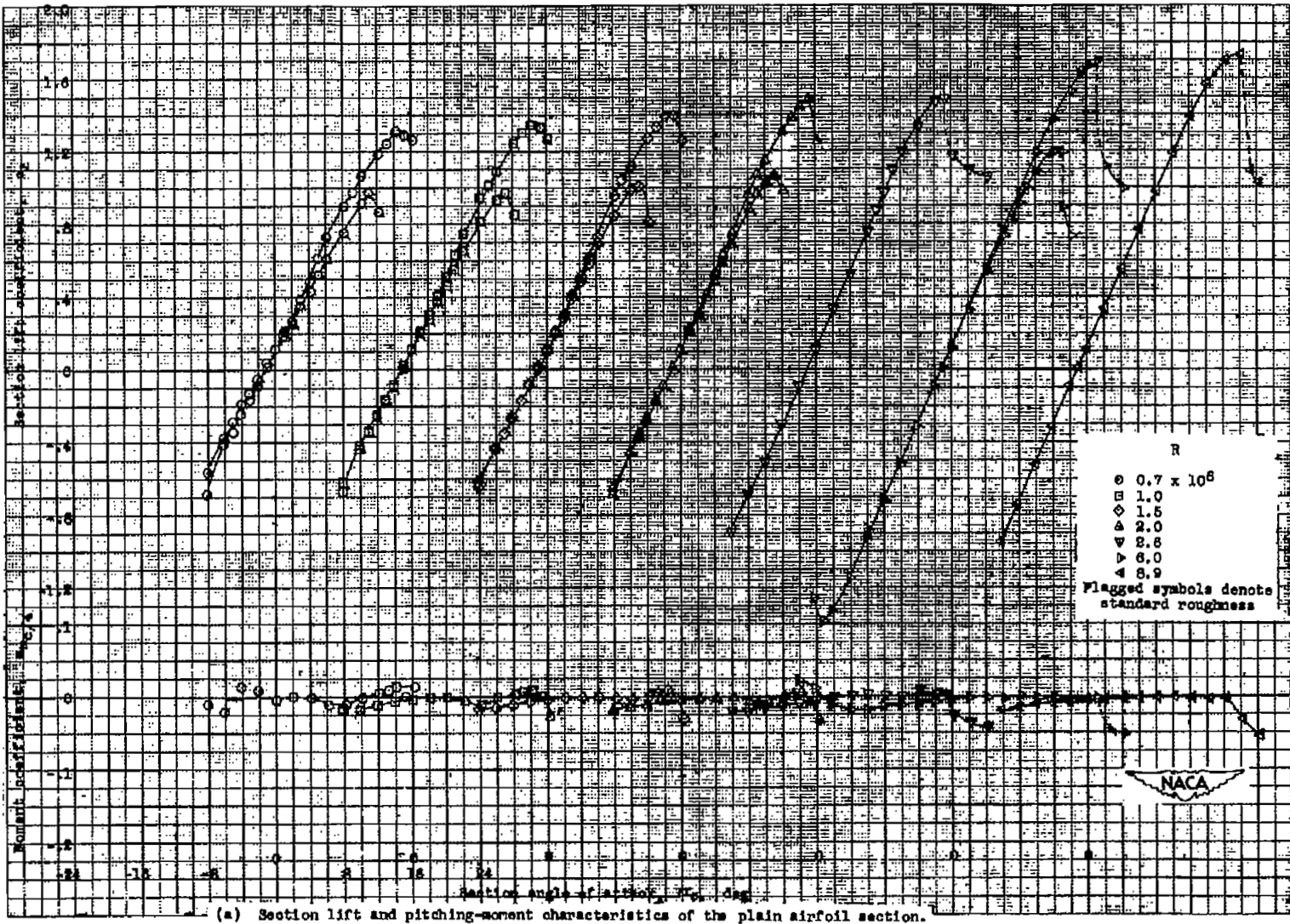
(b) Section lift and pitching-moment characteristics of the NACA 23012 airfoil section with a 0.20c simulated split flap deflected 60°.

Figure 5.- Continued.



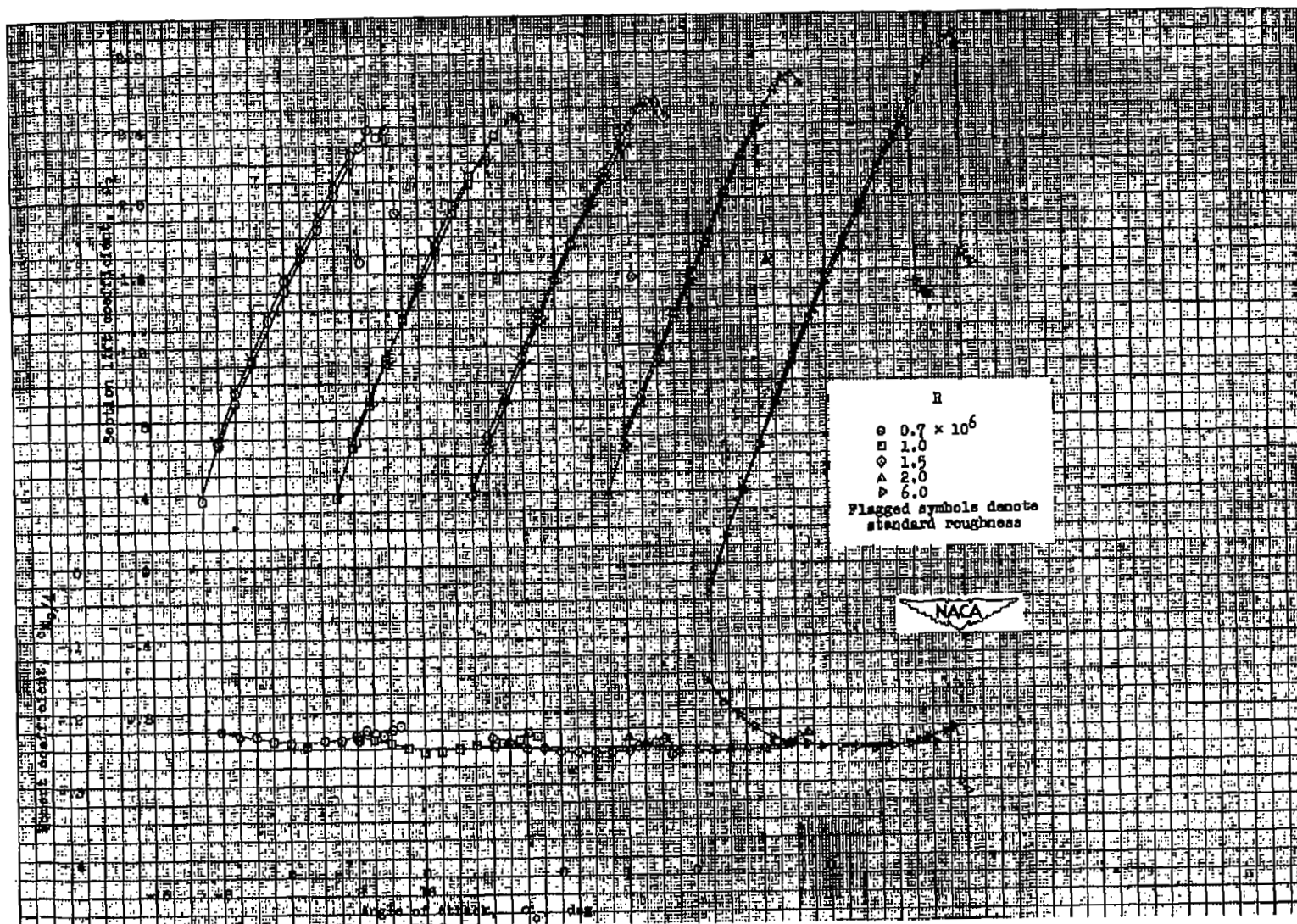
(a) Section drag characteristics and section pitching-moment characteristics about the aerodynamic center of the plain NACA 23012 airfoil section.

Figure 5.- Concluded.



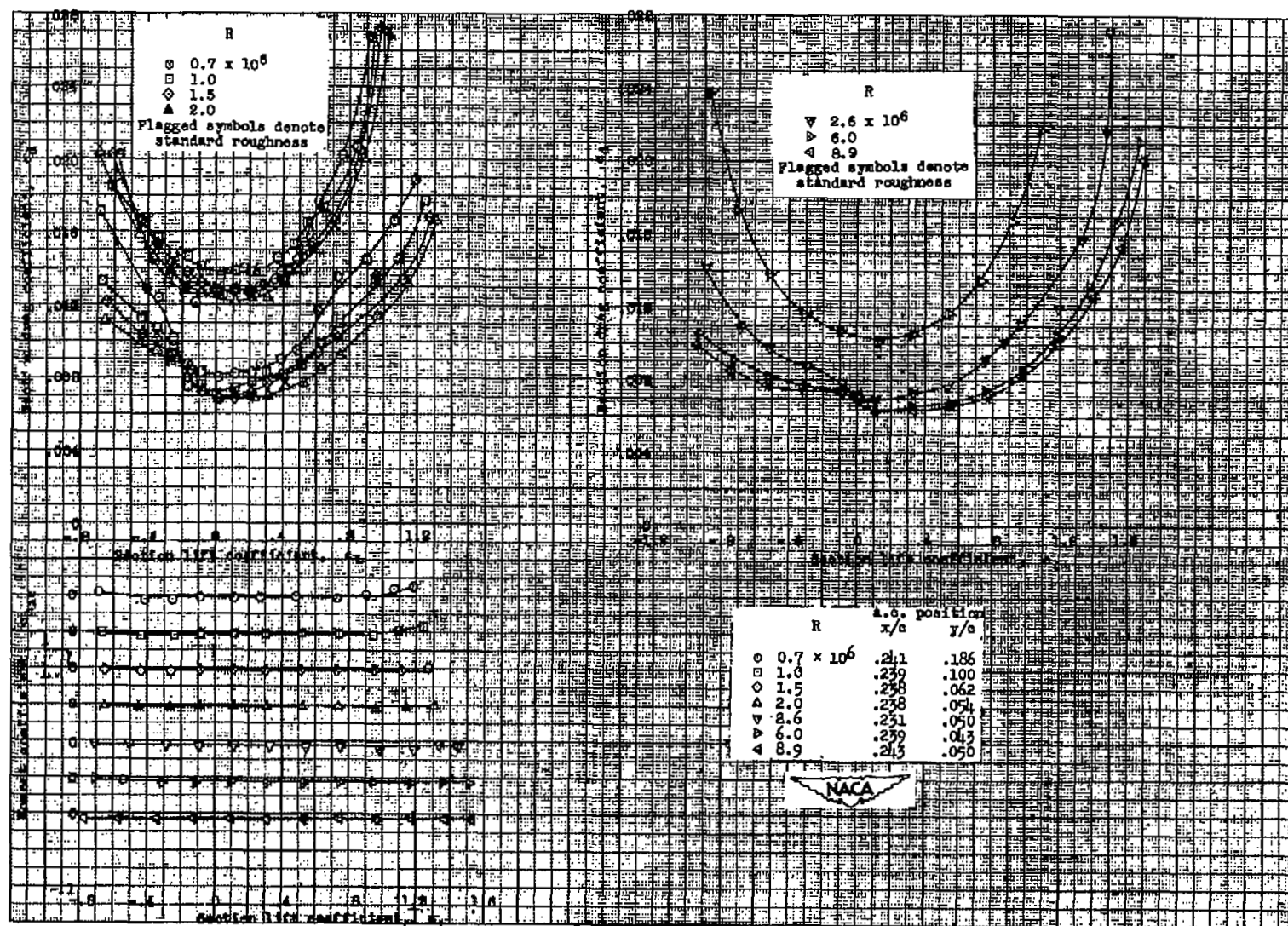
(a) Section lift and pitching-moment characteristics of the plain airfoil section.

Figure 6.- Aerodynamic characteristics of the NACA 23015 airfoil section, 84-inch chord. Tests, TDT 446, 450, 767, and LTT 451.



(b) Section lift and pitching-moment characteristics of the NACA 23015 airfoil section with a 0.20c simulated split flap deflected 60°.

Figure 6.- Continued.



(c) Section drag characteristics and section pitching-moment characteristics about the aerodynamic center of the plain NACA 23015 airfoil section.

Figure 6.- Concluded.

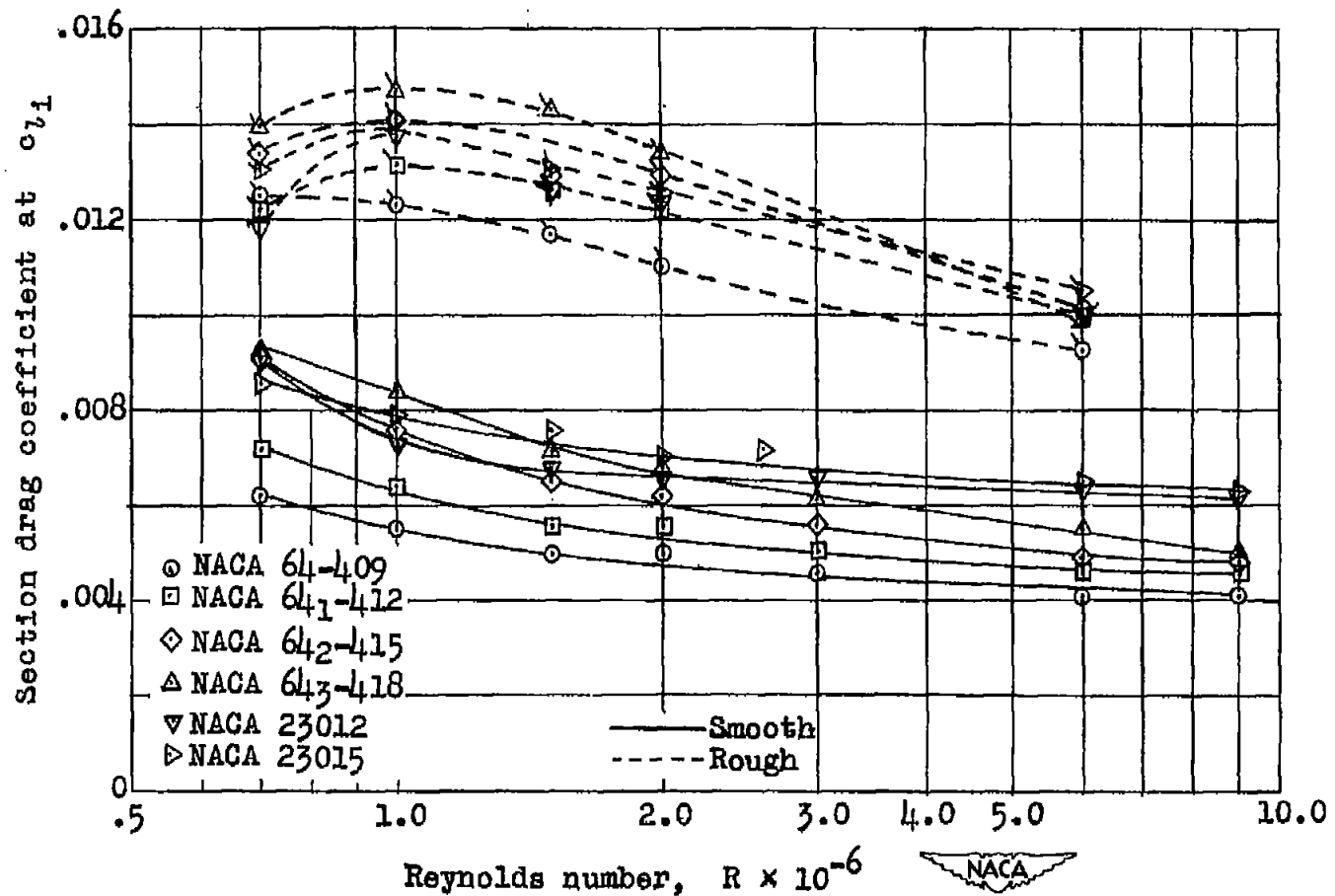
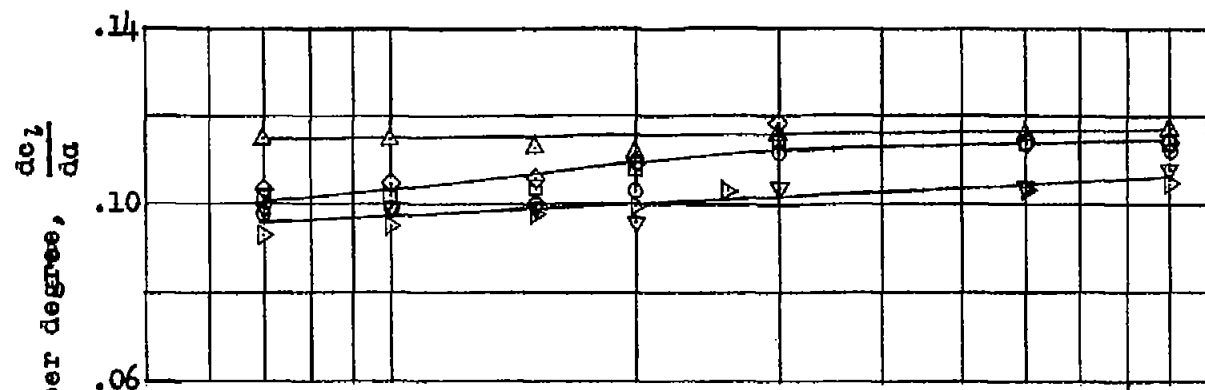
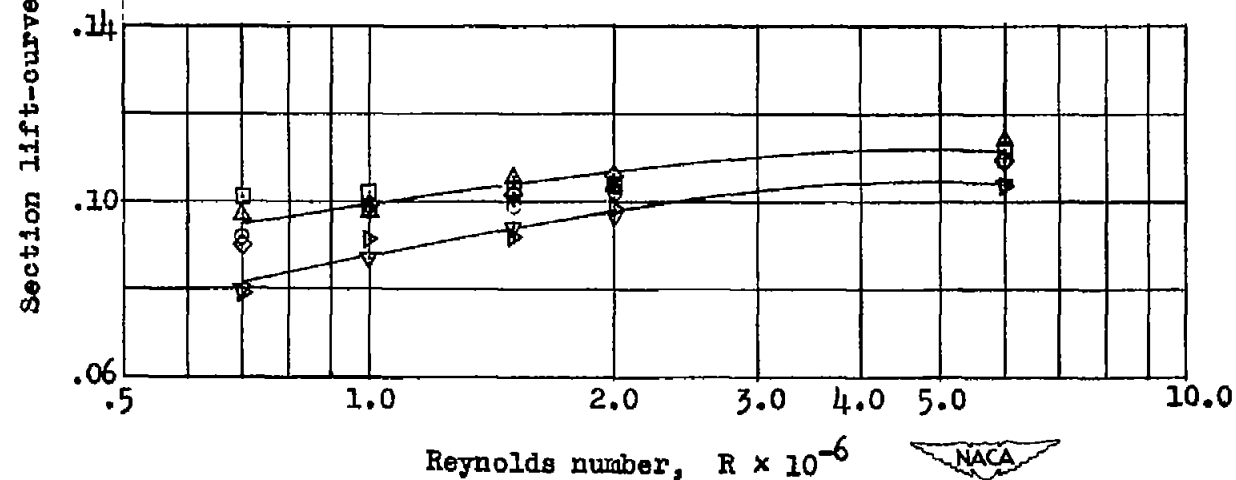


Figure 7.- Variation with Reynolds number of section drag coefficient at c_{l1} for a number of NACA airfoils, both in the smooth condition and with standard leading-edge roughness.



(a) Airfoils with smooth surfaces.



(b) Airfoils with standard leading-edge roughness .

Figure 8.- Variation of section lift-curve slope with Reynolds number for several NACA airfoil sections.

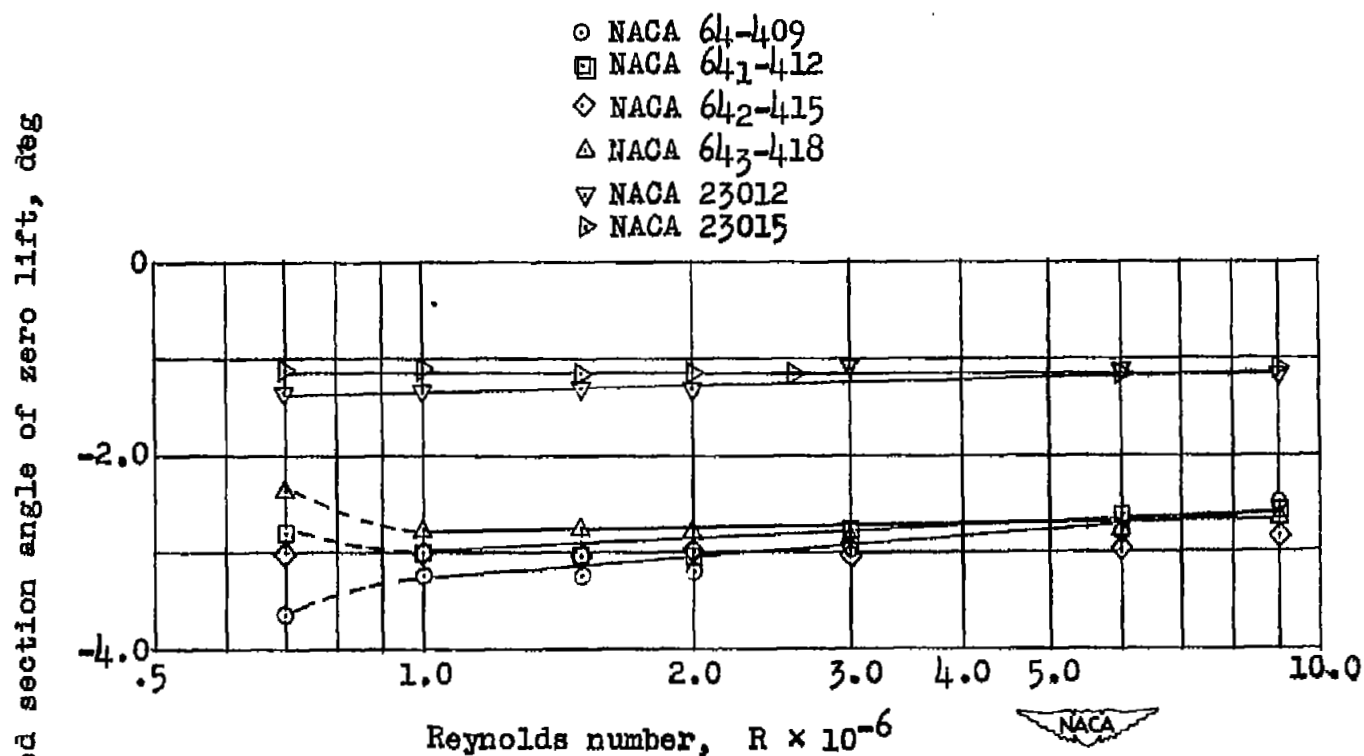


Figure 9.- Variation of section angle of zero lift with Reynolds number for several NACA airfoil sections with smooth surfaces.

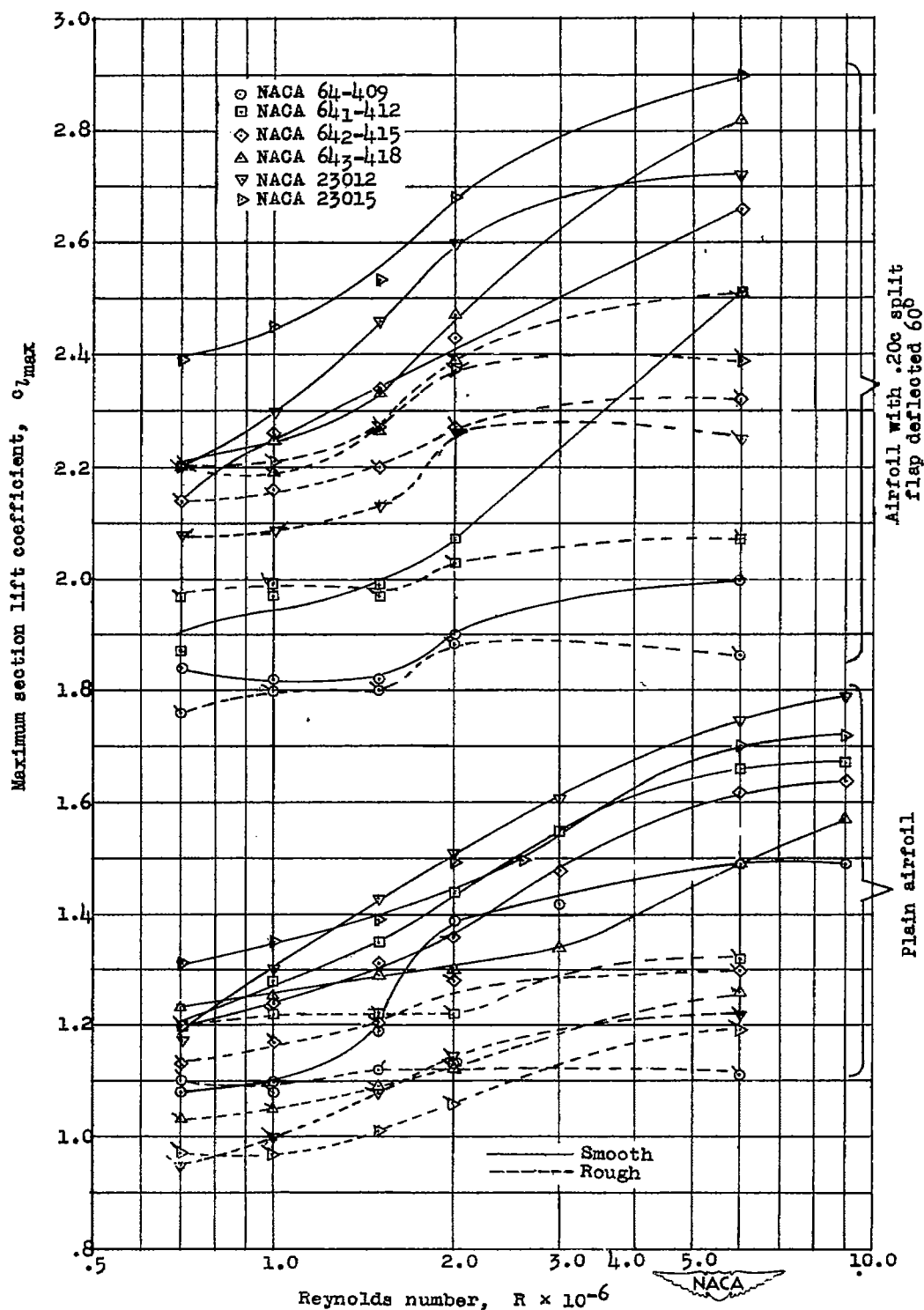


Figure 10.- Variation of maximum section lift coefficient with Reynolds number for a number of NACA airfoil sections both with and without split flaps and standard leading-edge roughness.